APPLICATION OF RESISTIVITY METHODS FOR GROUNDWATER EXPLORATION AROUND CHUKO, SOUTHERN REGION OF ETHIOPIA.

A THESIS PRESENTED TO THE SCHOOL OF

GRADUATE STUDIES

ADDIS ABABA UNIVERSITY

IN PARTIAL FULFILLMENT OF THE REQUIREMENTS FOR THE

DEGREE OF MASTER OF SCIENCE IN APPLIED GEOPHYSICS

by

Eyasu Bunaro

June 1998

ADDIS ABABA UNIVERSITY

School of Graduate studies

Application of Resistivity Methods for Groundwater Exploration Around Chuko, Southern Region of Ethiopia.

By

Eyasu Bunaro

Faculty of Science

Approved By :

Dr. Tilahun Mamo

(Examiner)

Mr. Abebe Ayele

(Examiner)

Dr. Tigistu Haile

(Advisor)

Mr. Taye Zewude

(Advisor)

Dr. Solomon Tadesse

(Chairman)

Acknowledgment

I acknowledge my indebtedness to Dr. Tigistu Haile and Ato Taye Zewude for following me at every step since the beginning of my work and for their concrete suggestions in finalizing the work. I acknowledge my deep gratitude to Dr. Tilahun Mamo and Dr. Solomon Tadesse for not only rendering their best help and cooperation but also encouraging and inspiring me all along.

I would be failing in my duty if I do not acknowledge my deep gratitude to all staffs of the Ethiopian Institute Geological Surveys (EIGS) for providing me all the necessary data, of the DAAD in country scholar ships for proving me funds for this research work, of the Geophysical Observatory, and of the Arbaminch Water Technology Institute for providing me the Terrameter SAS 300B resistivity measuring unit.

My thanks are also due to w/r Beshiwork Kidanewold for typing the paper and to all who helped me during this work. Last but not least I thank my Lord Jesus Christ for his grace.

contents

Abstract

Geophysical surveys and studies were carried out in southern Ethiopia around Chuko town for ground water exploration by the hydrogeological team in the Ethiopian Institute of Geological Surveys (EIGS) during 1984 - 1985. These data are reanalyzed from the scientific point of view. It is observed that the apparent resistivity data at a horizon having sufficient thickness can be described by the linear equation where the slope is the same as tangent of the dip angle of the fault.

The causes of the principles of equivalence for this particular survey area are aquifers (and possibly aquicludes) and this problem can be managed by fixing the resistivity value of aquifer known from other information sources such as wells. The results of the inversion shows that the resistivities of all layers associated with aquifers converges towards this fixed value without any change in the depth range indicating the fact that it is not the number of layers but the resistivity value of aquifer that is in the interpretation sounding curves for the ground water exploration. From type curve analysis the assumed faults are investigated which are identical with the ones obtained using profiling results. The type curve mapping is powerful in zone as well as fault mapping.

The stacked graphic plot, pseudoelectric and geoelectric section analysis shows that the resistivity of the water bearing formations are in general greater than 40 ohm-m and these formations, which are dominated by fractured volcanic rocks and sands of varying grain size, are most available in the eastern part of the base line with varying depth ranges.

Abstract

Geophysical surveys and studies were carried out in southern Ethiopia around Chuko town for ground water exploration by the hydrogeological team in the Ethiopian Institute of Geological Surveys (EIGS) during 1984 - 1985. These data are reanalyzed from the scientific point of view. It is observed that the apparent resistivity data at a horizon having sufficient thickness can be described by the linear equation where the slope is the same as tangent of the dip angle of the fault.

The causes of the principles of equivalence for this particular survey area are aquifers (and possibly aquicludes) and this problem can be managed by fixing the resistivity value of aquifer known from other information sources such as wells. The results of the inversion shows that the resistivities of all layers associated with aquifers converges towards this fixed value without any change in the depth range indicating the fact that it is not the number of layers but the resistivity value of aquifer that is in the interpretation sounding curves for the ground water exploration. From type curve analysis the assumed faults are investigated which are identical with the ones obtained using profiling results. The type curve mapping is powerful in zone as well as fault mapping.

The stacked graphic plot, pseudoelectric and geoelectric section analysis shows that the resistivity of the water bearing formations are in general greater than 40 ohm-m and these formations, which are dominated by fractured volcanic rocks and sands of varying grain size, are most available in the eastern part of the base line with varying depth ranges.

CHAPTER I

INTRODUCTION

1.1 General

The electrical conductivity of the earth materials can be studied by measuring the electrical potential distribution produced at the earth's surface by an electric current that is passed through the earth. In the most commonly used methods, direct current or low frequency alternating current is passed into the ground using a pair of electrodes, and the resulting distribution of the potential in the ground is measured by using another pair of electrodes connected to a sensitive voltmeter.

Assuming the subsurface medium to be homogeneous, it is possible to calculate the potential distribution and the path of the current flow from the knowledge of the electrode separations and from the magnitude of the current applied. However, the presence of a zone with anomalous resistivity, which may be due to discontinuity of a rock formation or change in its physical condition, perturbs the distribution of the current or potential lines, compared to their pattern in a homogeneous medium.

Since the earth's subsurface is not homogenous, the measured quantity in electrical resistivity method is the apparent resistivity, which is the representative of the ground under investigation.

The most commonly used configuration to measure apparent resistivity for the groundwater exploration is Schlumberger array for geolectrical sounding and half- Schlumberger array is thought to be the most effective for horizontal resistivity mapping.

The resulting geoelectrical sounding curves, which are plots of apparent resistivity versus electrode separation, can be interpreted in terms of resistivity and thickness of the individual layers using the curve matching techniques manually and /or by iterative procedures using computers. The resistivity profiling can also be interpreted in terms of resistivities and resistances of different zones at a given measuring depth.

The geoelectrical sounding curve alone can yield the information about the general structure of the subsurface, and when incorporated with other external information such as borehole data, other geophysical data, etc. can yield the fine structure or the specific arrangement of the strata of the area investigated. The results of the resistivity profiling give basically the information about lateral contacts, fault zones, fracturing of the lithologic units, etc.

Thus, from the measurements of potentials / potential gradient / curvature of potential on the surface i.e., from the measurement of the apparent resistivity on the surface, it is possible to know conditions and also the nature of subsurface layers. Accordingly, the electrical resistivity method has been successfully applied in the study of different geological problems. Specifically, it is very powerful in ground water exploration.

1.2. The Survey Area

1.2.1. Location and Physiography

Chuko town is situated on a flat plain at latitude 6°32'18" - 6 37' 17" N and longitude 38° 16' 51" - 38° 21'57" E along the Addis Ababa - Moyale highway. It is about 330 km from Addis Ababa and in the Southern region.

On either sides of the plain there are gullies and valley with water, although most of them are seasonal streams. The drainage system in this area is distributed widely, forming deep valley for drainage; and hence there is good flow of ground water to these valleys.

The inhabitants mainly depend on farming and the main crops are maize, coffee, fruits, inset, etc. and cattle raising. The location map of Chuko town and the neighboring area is shown in Fig.(1).

1.2.2. Geology and Hydrogeology

In general, the area is covered by a sedimentary (sandstone) limestone, clay, clay-sandy-clay) and volcanic rocks (ash, volcanic sands, ignimbrites, basalts, tuffs) of quaternary and neocene age.

Most of these rock units are horizontally stratified with strike direction, in general, N20°E. The top layer is a thick overburden material (unconsolidated alluvium sediments of volcanic origin like ash, weathered tuffs and weathered ignimbrites).

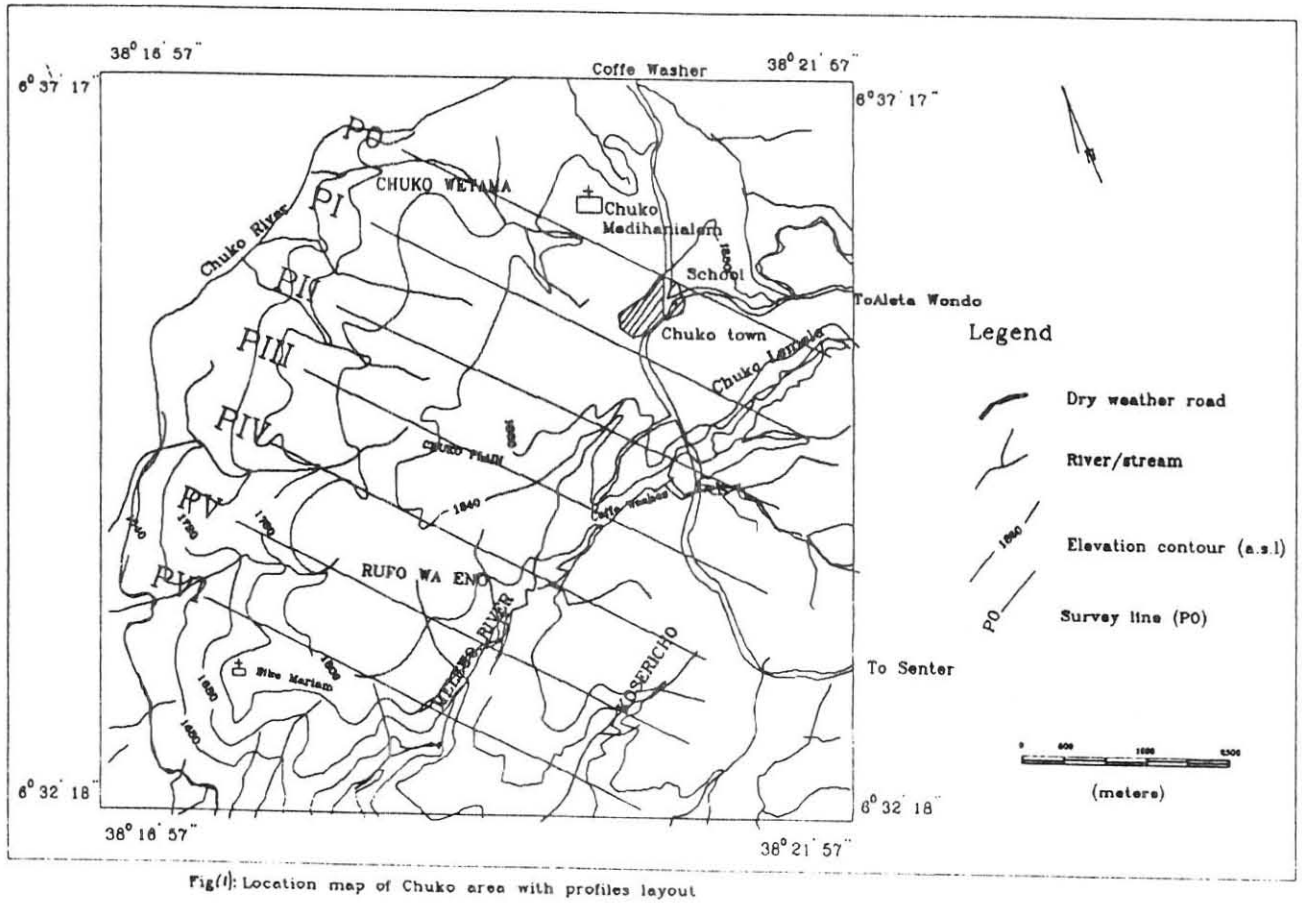

Fig(1): Location map of Chuko area with profiles layout

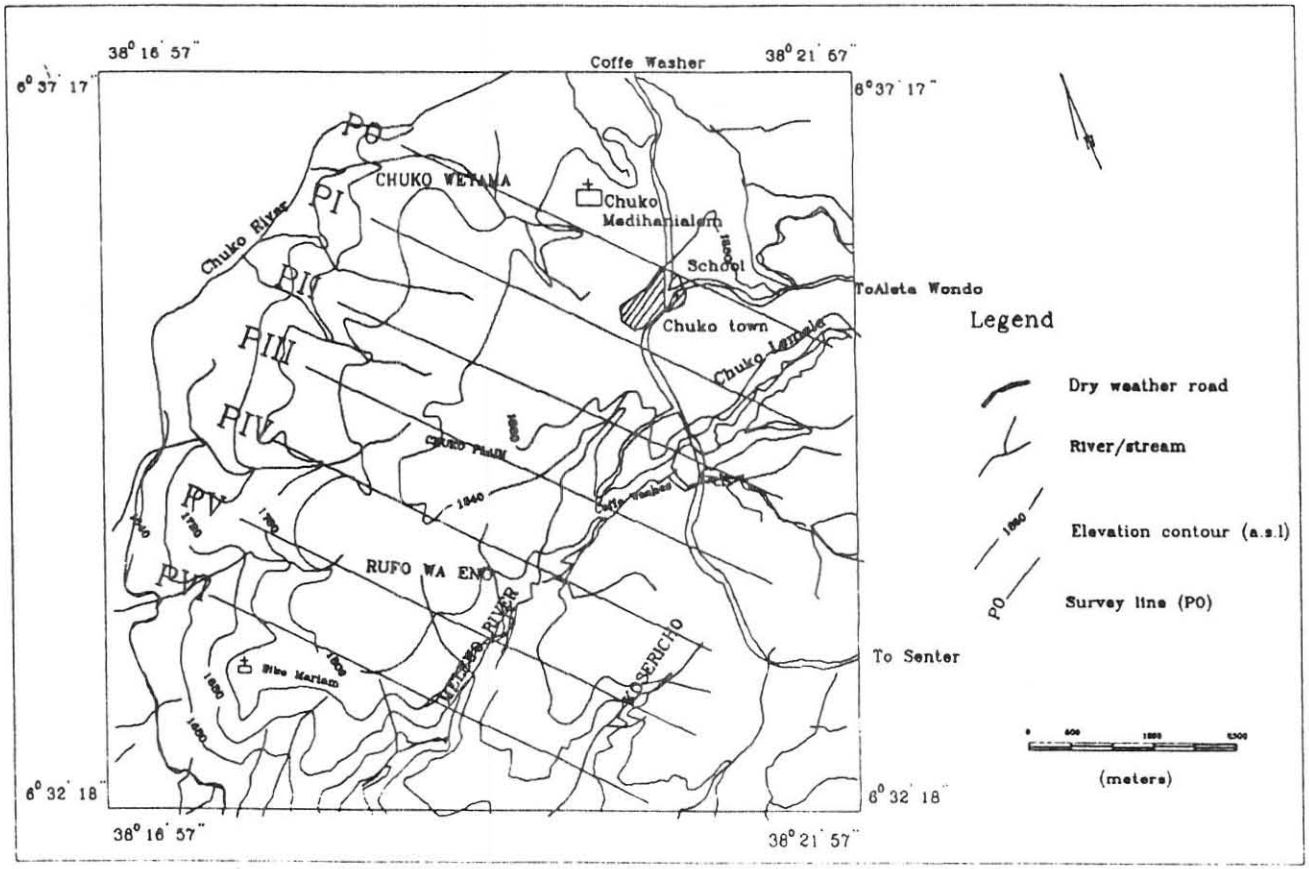

Fig(1): Location map of Chuko area with profiles layout

Underlying this top layer are compacted sedimentary (sandstone, limestone) and volcanic sand.

The main sources of drinking water are shallow (3-20 m) hand-dug wells, springs and streams. From the geological information from the existing bore-holes, clay and ignimbrites are assumed to be aquicludes, while volcanic sands, ash and gravely sand are thought to be good aquifers of the area. In some localities the iginimbrites might be fractured to be also relatively good aquifer zone.

1.3. General objectives of the work

A geophysical study was carried out around Chuko town by a hydrogeophysical team from the Geophysics Department of Ethiopian Institute of Geological surveys (EIGS) during 1984-1985. The methods employed were geoelectrical sounding, electrical profiling and magnetics. The geophysical data collected were processed manually and interpreted in correlation with the available geological log of existing two boreholes. Based on the preliminary results the team discussed various lithological units, tectonic faults and finally recommended six exploratory boreholes to be drilled.

In the present work the geoelectrical data were selected and these are believed to be sufficient for these research work. These data are analyzed manually as well as by iterative procedures with the aid of computers, and the results are interpreted in terms of lithologic units, tectonic faults and zones of aquifers and aquicludes.

The effects of the principle of equivalence were investigated in detail and some of the ways to manage these problems were suggested. The mathematical descriptions of profiling curves are formulated and the physical situations related to the formulation are described. The relevance's of type curves are discussed in detail.

Hence the objectives of this work include the following:

- to acquire practical experience in the interpretation of resistivity data.
- to develop geoelectrical models of a given area in terms of groundwater studies.
- to study the problem of equivalence using field data and recommend minimizing technique. Moreover,
- to determine the lithological succession and the possible water bearing horizons in terms of the resistivity and thickness (or depth).
- to locate tectonic faults and assist hydrogeological mapping using type curves.
- to drive the mathematical description of resistivity profiling data and to determine the relationships between the physical constants used in this formulation with the actual physical situation.

1.4. Methodologies Used

In order to achieve these objectives the resistivity methods, both vertical sounding and electrical profiling, were selected and applied in the field.

As shown in Fig.(1), a base line oriented N 20° E was laid parallel to the general strike direction of the geology of the area. Seven profiles each 6 km long were then laid perpendicular to this base line at spacing of 1km. The station interval for vertical sounding along each of these profiles was chosen to be 1km; and 100m station interval was chosen for the horizontal resistivity mapping.

Two mutually perpendicular vertical electrical soundings were conducted near the two-existing boreholes with a maximum separation of AB/2 = 500m.

A preliminary interpretation of these VES curves was made in order to determine a depth of interest to be mapped using resistivity profiling. The configuration applied for resistivity profiling was the half- Schlumberger, as shown in Fig.(7); and the appropriate separation chosen on the basis of the above VES information were AB/2 = 75m and MN/2 = 15m.

VES surveys were conducted using a Schlumberger array with a maximum separation of AB/2 = 500m.The direction of the spread of the configuration was along each profiles. The potential electrodes were displaced when the potential difference as read between the potential electrodes is low and the relationship between the potential and the current electrode separation used are that for AB/2 = 1.5-30m, MN/2 is fixed at 0.5m, AB/2 = 20-220m, MN/2 = 6m and AB/2 = 150 - 500m, MN/2 = 45m.

The instruments used for these geophysical surveys were the Indian Resistivity Unit of NGRI model with serial number 0.2-175 and a Russian Resistivity Unit of A-72, No.32012 model with serial number 106-78.

The total volume of work conducted in this area covered 48 line kms. However, due to the unavailability of data at some required points and also due to the unknown location of some VES points only the VES denoted by +, as shown in Fig.(10), are used for this work. Furthermore, no resistivity profiling is done over the fifth and sixth profiles and from the data from the boreholes VES data only the one indicated by BH in Fig.(10) is available. However, from these data different sets of the required maps are produced and hence it is believed that these data are sufficient for this research work.

CHAPTER II

THEORETICAL BACKGROUND

2.1. Potential distribution in the Earth

Resistivity is a physical property of a rock like density. However, the resistivity of rocks displays a wide range of values and is highly variable amongst all the physical properties of minerals and rocks. The reason is that in most rocks, electricity is conducted electrolytically by the interstitial fluid, and hence resistivity is controlled more by porosity, water content and water quality than by the resistivities of the rock matrix.

Resistivity is, therefore, an extremely variable parameter, not only from formation to formation but even within a particular formation. Thus there is no general correlation between rock lithology with resistivity. Nevertheless, resistivity methods allow one to determine the structure of the subsurface layers of the rock, the location of the groundwater table, the location of fault zones etc. These can be determined from the measurements of potential distribution in the earth's surface and from the geometric characteristics of the probe used to measure this distribution.

The electrical potential distribution for the direct current flow in a homogeneous medium satisfies Laplace's equation which is given by

$$\nabla^2 V = 0 \qquad (1)$$

The solution to this equation at the surface of homogeneous and isotropicearth at a

distance r from the point source offering a DC current of magnitude I is given by

$$V(r) = \frac{I\rho}{2\pi}\left(\frac{1}{r}\right) \qquad (2)$$

where ρ is the resistivity of the medium across which a current I flows, and since the function V(r) gives a semi-spherical surface r is the spherical variable.

In order to solve Laplace equation for the case of a layered earth, consider the medium to consist of finite number of layers separated from each other by horizontal boundary planes; each having a finite thickness except the deepest layer; and each being electrically homogeneous and electrically isotropic. We assume further that the field is generated by a point source of direct current that is located at the surface of the earth.

According to these specified conditions, the solution for the i^{th} layer in the cylindrical coordinate is given by

$$V_i(r,z) = \frac{I\rho_1}{2\pi}\int_0^\infty \left[e^{-pz} + A_i(p)e^{-pz} + B_i(p)e^{pz}\right]J_0(pr)\,dp \qquad (3)$$

where z is the coordinate axis in the downward vertical direction, r is the cylindrical variable, A_i (p) and B_i (p) are the integration constants, $\rho 1$ is the resistivity of the first layer and J0(pr) is the Bessel function order zero. This integral is called the Stefanescu's Integral.

The integration constants A_i (p) and B_i (p) can be obtained from the following boundary conditions:

a) At each of the boundary planes the potential and the vertical component of current density must be continuous.

b) For the earth - air boundary the vertical component of the current density is zero. This leads to $A_1(p) = B_1(p)$

c) In the deepest layer, for the n-layered earth, $B_n(p) = 0$ because the potential at infinity is zero.

These results in the 2n equations in order to determine the 2n unknown functions $A_i(p)$ & $B_i(p)$. In the resistivity method we are only interested in the potential at the earth's surface and it therefore suffices to determine $A_1(p)$.

The potential in the first layer is given, from equation (3) , by

$$V_1(r,z) = \frac{I\rho_1}{2\pi}\int_0^\infty \left[e^{pz} + A_1(p)\left\{e^{-pz} + e^{pz}\right\}\right] J_o(pr)\,dp \qquad (4)$$

At the earth's surface z = 0, and after setting $V_1(r,0) = V(r)$ this equation becomes

$$V(r) = \frac{I\rho_1}{2\pi}\int_0^\infty \left[1 + 2A_1(p)\right] J_o(pr)\,dp \qquad (5)$$

Letting $K(p) = 1 + 2A_1(p)$ (6)

into equation (5) we have

$$V(r) = \frac{I\rho_1}{2\pi}\int_0^\infty K(p)\,J_o(pr)\,dp \qquad (7)$$

(The function K(p) has been introduced into the resistivity theory by Slichter (1933) and referred to as Slichter's kernel function; where as the function $A_1(p)$ is referred to as the Stefanescu Kernel function)

Another simple method of finding A_1 (p) is the recurrence relation, known as the Pekeris recurrence relation given by

$$K_i(p) = \frac{K_{i+1} + q_i \tanh(ph_i)}{q_i + K_{i+1} \tanh(ph_i)} \quad (8)$$

where K_i (p), ρ and h_i are the K - function, resistivity and thickness of the i^{th} layer, respectively and $q_i = \rho_i/\rho_{i+1}$. Hence, from the known layer distribution parameters and from the known K - function in the substratum (n^{th} layer), K_n (p) = 1 because in the substratum A_1 (p) = 0, the recurrent application of equation (8) gives the value of the K-function in all other layers: K_{n-1} (p), K_{n-2} (p), ..., K_2(P) and K_1(p) where K_1 (p) denotes K (p). Hence using equations (8) and (6) we can determine A_1 (p).

Koefoed (1970) introduced the "resistivity transform function", denoted by T_i(p), which is defined by the equation

$$T_i(p) = \rho_i K_i(p) \quad (9)$$

where the subscript has the same meaning as before. Expressed for the resistivity transform, the Pekeris recurrence relation are

$$T_i(p) = \frac{T_{i+1} + \rho_i \tanh(ph_i)}{1 + \left(\frac{T_{i+1}}{\rho_i}\right) \tanh(ph_i)} \quad (10)$$

Using this we can find the values of T-function in each layer: T_{n-1} , T_{n-2} ,....,T_2 & T_1 where T_1 (p) = T(p) is the T- function at the earth's surface.

Hence equation (7) can be expressed in terms of T(p) as

$$V(r) = \frac{I}{2\pi} \int_0^\infty T(p)\, J_0(pr)dp \qquad (11)$$

Then once the T-function is known it could be used to determine the resistivities and thicknesses of the layers using equation (10).

2.2. Practical Calculations of Apparent Resistivities

In the previous considerations we have assumed a single current source to produce potential distribution in a medium. However, in practice, current is introduced into the ground by two current electrodes; not by one: the source and the sink. Conventionally the source gives rise to a positive potential and the sink gives rise to a negative potential. Hence, the resultant potential at an observation point "0", r_1 distance away from the source and r_2 distance away from the sink, at the surface of homogeneous and isotropic earth with resistivity ρ is given, according to equation (2), by

$$V(O) = V(r_1) - V(r_2) \qquad (12)$$

However, in practice, one can not measure the potential at a point but the potential difference between two points. For this purpose we consider a generalized four electrode configuration in which a direct current I is introduced into the ground through two electrodes C_1 (or A) and C_2 (or B) (also known as current electrodes) and then the measurement of the potential difference between any two points P_1 (or M) and P_2 (or N) is made by the two electrodes placed at P_1 and P_2 (also known as the measuring electrodes or the potential electrodes).

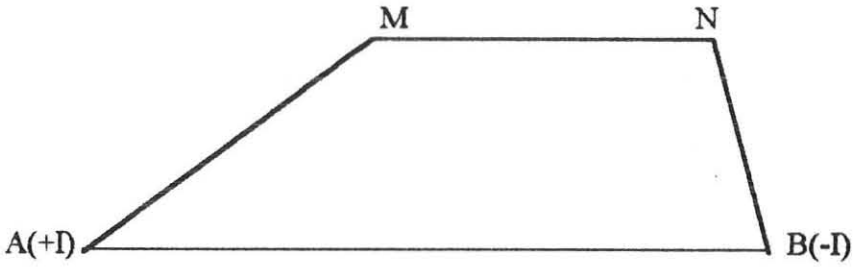

Fig.(2): Generalized Four Electrode Array

The potential difference between M and N is given by

$$\Delta V = V(M) - V(N) \tag{13}$$

where, according to equation (12)

$$V(M) = \frac{I\rho}{2\pi}\left(\frac{1}{AM} - \frac{1}{BM}\right) \;\&\; V(N) = \frac{I\rho}{2\pi}\left(\frac{1}{AN} - \frac{1}{BN}\right) \tag{14}$$

Substituting these into equation (13) we get

$$\Delta V = \frac{I\rho}{2\pi}\left[\frac{1}{AM} - \frac{1}{BM} - \frac{1}{AB} + \frac{1}{BN}\right] \tag{15}$$

After rearranging can be written in the form

$$\rho = G\,\frac{\Delta V}{I} \tag{16}$$

where $$G = \frac{2\pi}{\left[\frac{1}{AM} - \frac{1}{BM} - \frac{1}{AN} + \frac{1}{BN}\right]} \tag{17}$$

is the characteristic of an electrode configuration, depending on current distribution and position of potential electrodes and is called the geometric factor (or geometric coefficient) of an array.

For example, for the symmetrical configuration in which the four electrodes are positioned symmetrically along a straight line, with the current electrodes on outside and the potential electrodes on inside so that AM = BN = (AB - MN)/2 and AN = BM = (AB + MN)/2 the geometric factor in equation (17) reduces to

$$G = \frac{\pi\left[\left(\frac{AB}{2}\right)^2 - \left(\frac{MN}{2}\right)^2\right]}{MN} \qquad (18)$$

Hence, the resistivity of the subsurface can be measured from the measurements of the potential difference and the knowledge of the geometry of the electrode layouts. In the case of a homogeneous and isotropic earth, the value of ρ represents the true resistivity of the subsurface. However, its value will never be equal to the true resistivity if the medium below an array is not homogeneous and in this case ρ must be the representative of the true resistivities of the various layers constituting the given subsurface formation. To account for this a quantity known as the "apparent resistivity and denoted by ρ_a", is defined in such a way that it is equal to the true resistivity of a fictitious homogeneous and isotropic medium which gives the same potential difference for the same current and same electrode layouts. Thus, for the layered earth equation (16) is more appropriately written as

$$\rho_a = G\frac{\Delta V}{I} \qquad (19)$$

This apparent resistivity is the one that one gets from field measurements of G, ΔV and I (i.e., it is the observed value or the result of field measurement). But its value alone does not suffice for the determination of layer parameters if the ground is inhomogeneous. The layer parameter determination also makes use of the theoretically computed apparent resistivity values. This theoretical apparent resistivity function on logarithmic scale is given by

$$\rho_a(x) = \int_{-\infty}^{\infty} T(y)\, f(x-y)\, dy \qquad (20)$$

where f(x) is called the resistivity filter function and T(x) is called the resistivity transform function. This is a convolution integral

$$\rho_a(x) = T(x) * f(x) \qquad (21)$$

where "*" denotes the convolution operator.

This fact indicates the possibility of applying the method of digital linear filtering in resistivity theory in which the values of one of the functions are obtained as a linear expression in the sample values of the other function, the samples being taken at a constant interval along the abscissa axis, say Δx. The coefficients in this linear expression are called the filter coefficients.

The observed apparent resistivity values given in equation (19) and the theoretically computed apparent resistivity values using equation (21) are used for the iterative procedures in the interpretation of the resistivity data.

2.3. Exploration principles and procedures

There are two different types of geoelectric prospecting: "geoelectric depth sounding" and "geoelectric mapping or profiling", also called "vertical" and "horizontal" electrical exploration.

Geoelectric depth sounding (or vertical electrical sounding, VES) will be applied when the ground is nearly horizontally stratified such as is the case in undisturbed sedimentary basins; and one wishes to determine the depth to the different layers. The basic principle is that the farther away from a current source the measurement of the potential difference is made, the deeper the probing by the current will be.

The most commonly used configuration for VES is the Schlumberger Configuration which is one of the symmetrical arrangements. In order to change the depth of penetration, the current electrodes are displaced outward after every measurement whereas the potential electrodes are occasionally displaced when the ratio AB : MN is too large so that the potential difference becomes too small to be measured otherwise, the potential electrodes are fixed in a given position. Specifically the electrode separations AB and MN must satisfy the condition that AB $\geq$5 MN so that when MN is changed this relation still holds. Two readings are necessary when the separation between M and N is changed.

In VES, the electrode spacing are increased at constant (logarithmic) intervals and the value of apparent resistivity is plotted as a function of electrode spacing (on logarithmic coordinate paper).

The curve of ρ_a versus AB/2 is called an electrical sounding curve. The comparison of electrical sounding curve at neighboring VES points is particularly helpful in the study of slowly varying bed depths and resistivities in an earth where the bedding is horizontal or slightly dipping.

The same set of VES measurements along a given profile can be grouped to best serve the problem in question. In one case, they may be grouped into a succession of electrical soundings, and in the other case into a set of horizontal resistivity variations at different depths of investigation. However, the investigation of a band of earth with a given depth and given width is best carried out if one moves the configuration of fixed length along a profile. If the procedure is repeated, with parallel profiles properly spaced, a whole slice of earth with the given thickness would have been investigated. This method of prospecting is called horizontal electrical resistivity profiling or mapping. In resistivity mapping one or two constant electrode spacing are chosen according to the desired depth of investigation, which may be chosen on the basis of VES, borehole or other information, and the whole configuration is moved to different points along profile(s).

Any of the electrode arrays used in VES may be used in horizontal profiling measurements. The parameter measured will be the apparent resistivity and the value of apparent resistivity is plotted, generally, at the geometric center of the electrode configuration in linear scale, and the results are presented as apparent resistivity profiles or maps.

This map then groups the results corresponding to a given depth of investigation and will reflect the lateral variations of resistivity within the slice of earth included in the measurement (maximum apparent resistivity anomalies are obtained at right angles to the strike of the geologic structure). By comparing a series of such maps, each corresponding to a different depth of investigation, one could determine the variation of resistivity with depth. However, the variation with depth would be easier to study using VES, as discussed above.

In profiling it is strongly recommended that at least two different electrode spacing be used at each station in order to aid in distinguishing the effects of shallow geologic structures from the effects of deeper ones.

In the field, a sounding is normally done first, because it is necessary to have a relatively quick and easy method of obtaining a rough and preliminary interpretation of the data so that a depth of investigation for profiling can be determined. The most appropriate and the most often used method of interpretation for this purpose is the two-layer plus auxiliary curve method, which will be discussed in section 3.1.2.

2.4. Interpretation of Resistivity Data

2.4.1. VES Data Interpretation Methods

The interpretation of VES data can be carried out using: the manual interpretation procedures using theoretical curves and/or the automatic interpretation procedures using computers and appropriate software.

a) Manual (Curve Matching) Techniques

The analytical expressions of apparent resistivity for a given array, Schlumberger array in our case, can be obtained, in principle, for any number of layer distributions. We can then plot the ratio ρ_a/ρ_1 versus $AB/2h_1$, where ρ_1 and h_1 are the resistivity and thickness of the first topmost layer, on double logarithmic scale. On the ordinate axis the log ρ_a/ρ_1 is plotted and on the abscissa log $AB/2h_1$ is plotted. The resulting theoretical curves are then called master curves or standard curves.

The field curves, that are going to be interpreted with the help of these standard curves, are a plot of the observed or measured apparent resistivity ρ_a , over a wide range of electrode spacings AB/2 in the case of Schlumberger array, on logarithmic interval. The field curves are drawn on a transparent paper with the same modulus as that of the standard curves. The number of inflections in the field curve indicate the number of layers explored by the resistivity method.

The interpretation consists of matching the field curves with one of the master curves. Matching is done by moving the field curves over the master curves keeping the coordinate axes parallel; and the match gives the model of the earth under investigation. If no matching can be obtained, this indicates that the wrong model have been chosen.

The two-layer standard curves are used for two-layer distributions, the three-layer standard curves are used for three layer distributions and so on. Master curves to a maximum of four layers are available. For more layers none of these master curves are applicable and hence the curve matching is not practical anymore. However, to overcome this problem auxiliary curves are constructed so that any number of layers can be interpreted. The one most often interpretation procedure involves the use of the two-layer master curves plus auxiliary curves based on the assumption that any three-layer resistivity section can be analytically expressed as an equivalent two-layer section, and so on.

This method may be briefly described as follows. Each of the apparent resistivity curve is approximated by a two-layer apparent resistivity curve; and the coordinates of the cross of this two-layer curve are considered to represent the thickness and resistivity of a fictitious layer that replaces the sequence of shallower layers. The procedure for the interpretation of the general curves with the layer distribution given by $\rho_1 > \rho_2 > \rho_3 < \rho_4 < \rho_5 > \rho_6$ which is the QHAK-type curve is presented as follows:

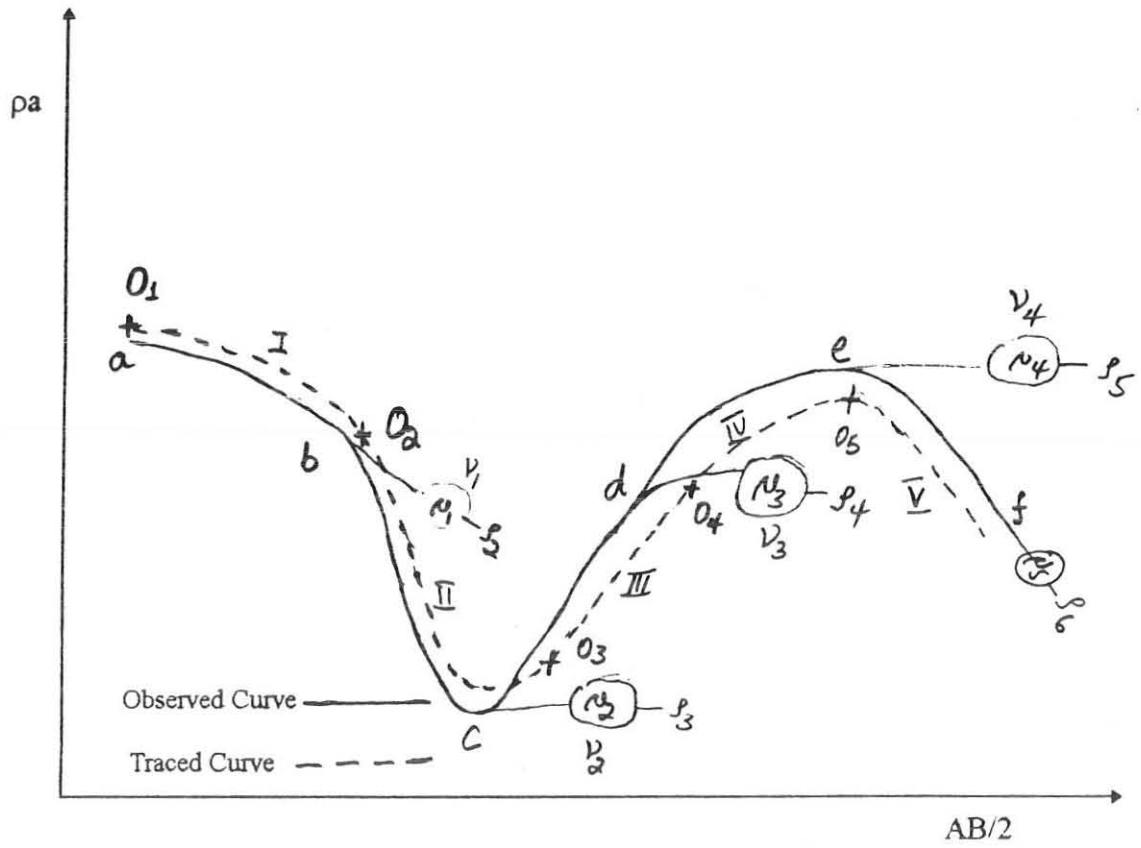

Fig.(3): Six-layer example for two-layer graphical analysis

(Observed or field curve)

where the symbol + in this figure denotes any of the i^{th} coordinate point $O_i = (h_{ei}, \rho_{ei})$ where h_{ei} and ρ_{ei} respectively are the equivalent thickness of the $(i-1)^{th}$ and i^{th} layers resistivity of the $(i-1)^{th}$ and i^{th} layers; and the coefficients μ and ν are defined as follows: $\mu_i = \rho_{i+1}/\rho_i$ and $\nu_i = h_{i+1}/h_i$.

1) Plot apparent resistivity versus the electrode spacing of the on a semi-transparent log-log paper of the same scale as the standard curve and auxiliary curve.

For the sake of convenience let us denote the curves as follows:

Observed Curve : OB (Fig(3))

Standard Curve : SC (Fig(4))

Auxiliary Curve of K-type : AC-K (Fig(5a))

" " " Q-type : AC-Q (Fig(5b))

" " " A-type : AC-A (Fig(6a))

" " " H-type : AC-H (Fig(6b))

2) Overlay OB on the SC and move it to its own axis down and side ways until a-b portion of OB is best matched by a section of SC. Mark the location of the SC origin onto OB plot with coordinate point $O_1 = (h_{e1}, \rho_{e1})$ and read the value of the coefficient μ_1 of the matching SC. This give the resistivity of the first and second layers and the thickness of the first layer: $h_{e1} = h_1$, $\rho_{e1} = \rho_1$ and $\rho_2 = \mu_1 \rho_{e1}$.

Since the two-layer standard curves plus auxiliary curves method is based on the assumption that any three-layer resistivity section can be analytically expressed as an equivalent two-layer section, we have to assume the three-layer section a-b-c as a two-layer section so that the segment b-c can be interpreted. This is possible if we consider the first two-layers as one layer with equivalent thickness h_{e2} and equivalent resistivity ρ_{e2}. In order to perform this operation, since a-b-c has resistivity distribution $\rho_1 > \rho_2 > \rho_3$ which is Q-type curve, we put O_1 on the origin of the AC-Q with axes being parallel and then trace the AC-Q curve with value μ_1 onto the OB plot (the trace I shown in Fig. (3)).

3) Again place OB onto SC and move it to its own axis down and side ways keeping the origin of the SC along the traced curve I until a best match of b-c is obtained. Mark the origin of SC on the OB plot and denote it by $O_2 = (h_{e2}, \rho_{e2})$ and read the μ_2 value of the matched SC curve. From these we can find $\rho_3 = \mu_2 \rho_{e2}$. To find h_2 , put O_1 of the OB plot onto the origin of AC-Q and read the value of vertical line where O_2 lies. This gives ν_1 so that $h_2 = \nu_1 h_{e1}$.

Now to proceed to interpret the c-d portion of OB we have to use the basic assumption of the two-layer plus auxiliary point method. The three-layer section b-c-d ($\rho_2 > \rho_3 < \rho_4$: H-type curve) can be reduced to the equivalent two-layer section if we assume the second and third layers as one fictitious layer with resistivity ρ_{e3} and thickness h_{e3} . In order to do this we put O_2 on the origin of AC-H with axes of both being parallel, and then trace the AC-H curve with value μ_2 on to the OB plot (the trace II as shown in Fig, (3)).

4) Now place OB onto SC and move OB while keeping axes of both parallel and also keeping the origin of SC along the trace II until the c-d portion is best matched with one of the SC curves. Mark the origin of SC onto OB plot $O_3 = (h_{e3}, \rho_{e3})$ and read the value of μ_3 of the matched SC curve. This gives $\rho_4 = \mu_3 \rho_{e3}$. To find h_3 , put O_2 onto the origin of AC-H while keeping the axes of both being parallel and read the value of the vertical line at which O_3 lies. This gives ν_2 so that $h_3 = \nu_2 h_{e2}$.

Again we have to use the basic assumption of the two-layer plus auxiliary point method in order to interpret the d-e portion of the OB plot. If we assume the third and fourth layers as one fictitious layer with resistivity ρ_{e4} and thickness h_{e4}, then the three-layer section c-d-e ($\rho_3 < \rho_4 < \rho_5$: A-type curve) is reduced to the equivalent two-layer section. In order to do this we put O_3 at the ordinate point with value μ_3 onto the OB plot (trace III as shown in Fig. (3)).

5) Place OB onto SC and, while keeping the origin of SC along the trace III and also axes of both parallel, shift OB until the d-e portion is best matched with one of the curves of SC. Mark the origin of SC onto OB plot $O_4 = (h_{e4}, \rho_{e4})$ and read μ_4 of the matched SC so that $\rho_5 = \mu_4 \rho_{e4}$. To find h_4 , put O_3 on the ordinate point of AC-A with value μ_3 , keeping the axes of both being parallel, and read diagonally the value of the curve at which 0_4 lies. This gives ν_3 so that $h_4 = \nu_3 h_{e3}$.

In order to interpret the e-f portion we use the basic assumption of the two layer plus auxiliary point method by assuming the fourth and fifth layers as one fictitious layer with resistivity ρ_{e5} and thickness has so that the three-layer section d-e-f ($\rho_4 < \rho_5 > \rho_6$: K - type curve) is reduced to the equivalent two-layer section. To do this we put O_4 on the ordinate point with value μ_4 of the AC-k, while the axes of both parallel, and then trace the Ac-k curve with value μ_4 onto the OB plot (trace IV in Fig. (3)).

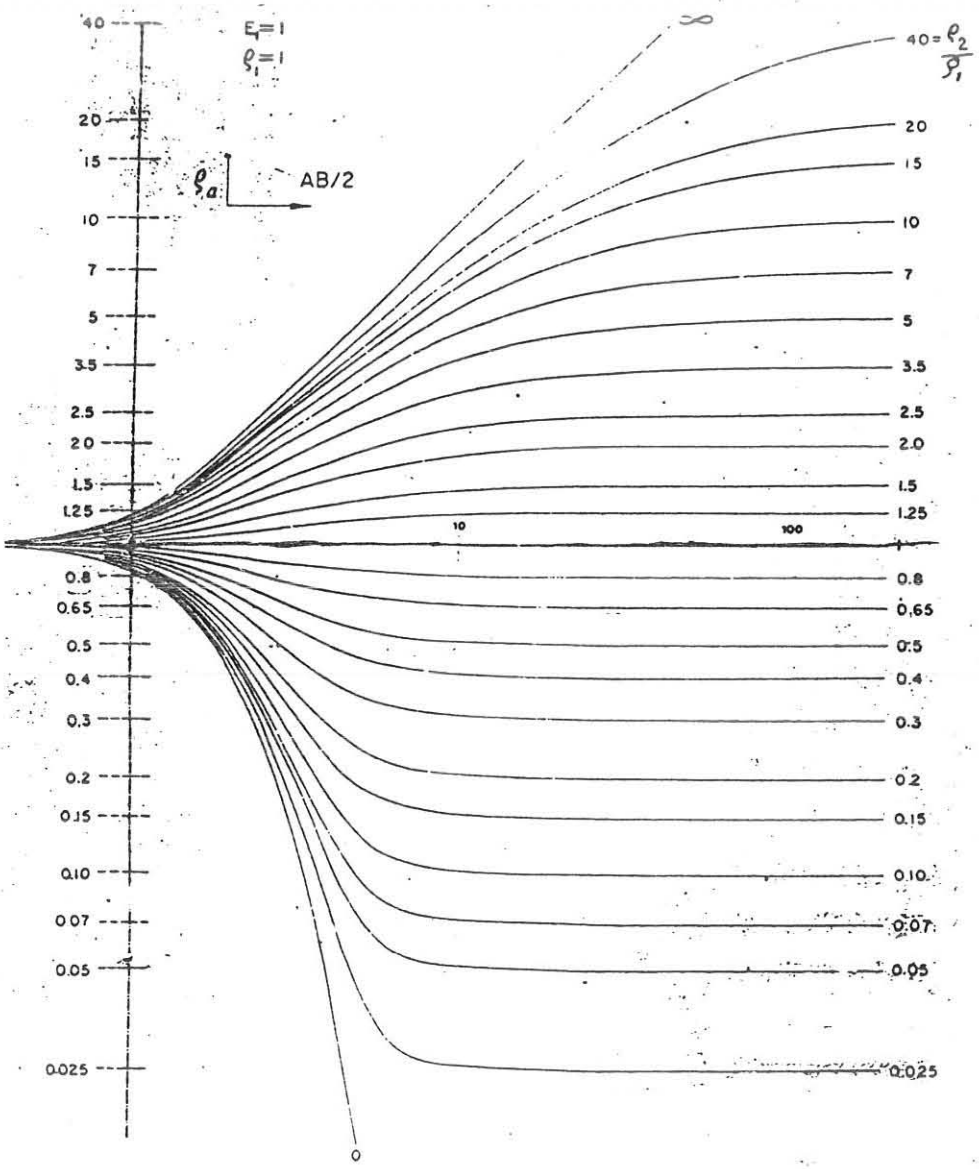

Fig(4)

TWO-LAYER CURVES

AUXILIARY GRAPH (K-TYPE)

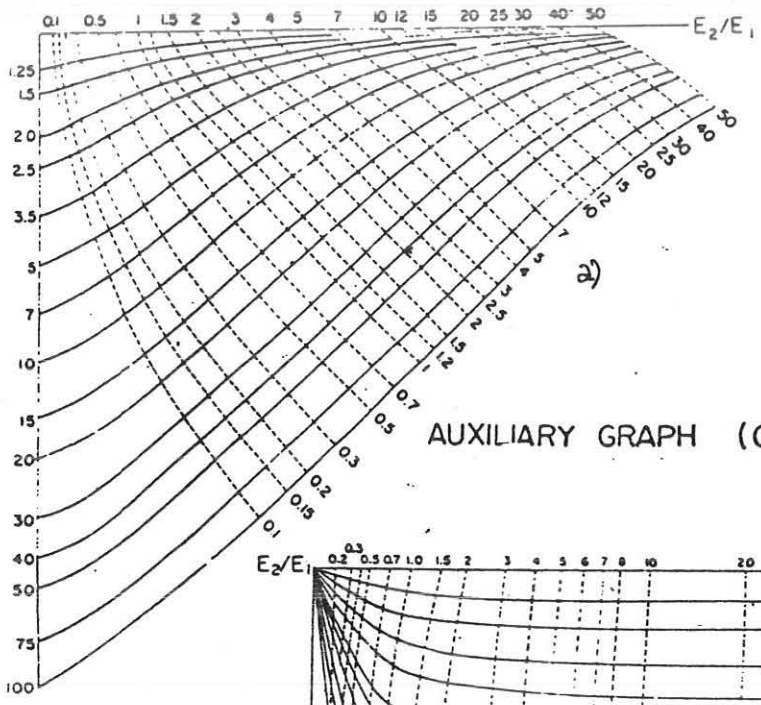

AUXILIARY GRAPH (Q-TYPE)

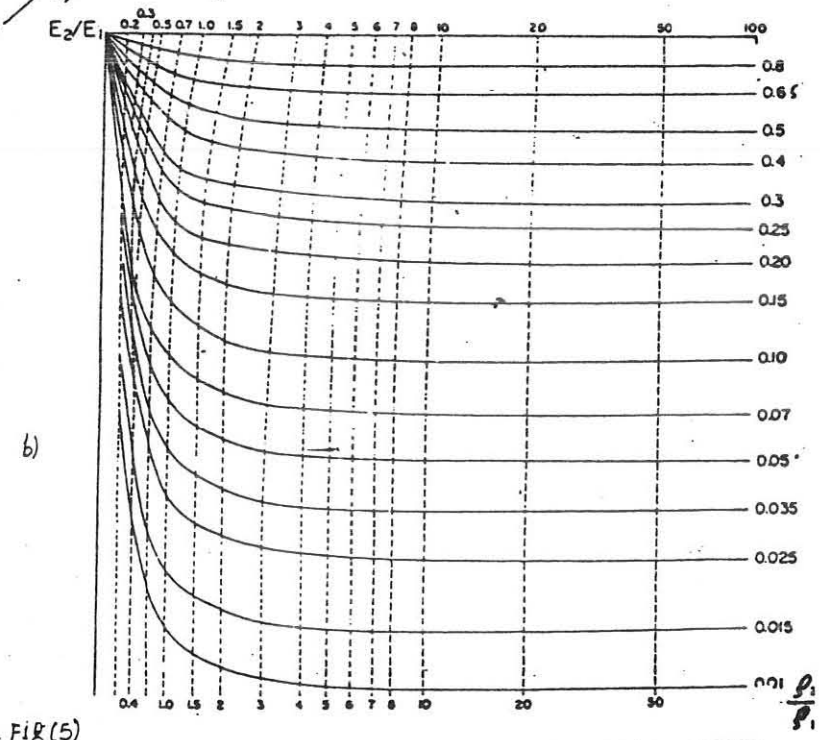

Fig (5)

ORELLANA-MOONEY

AUXILIARY GRAPH (A-TYPE)

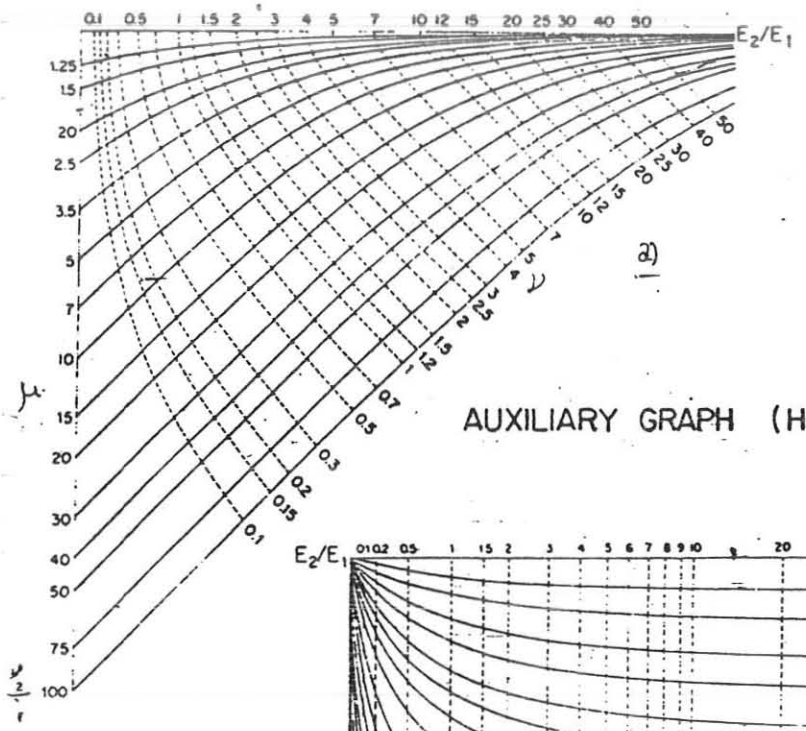

AUXILIARY GRAPH (H-TYPE)

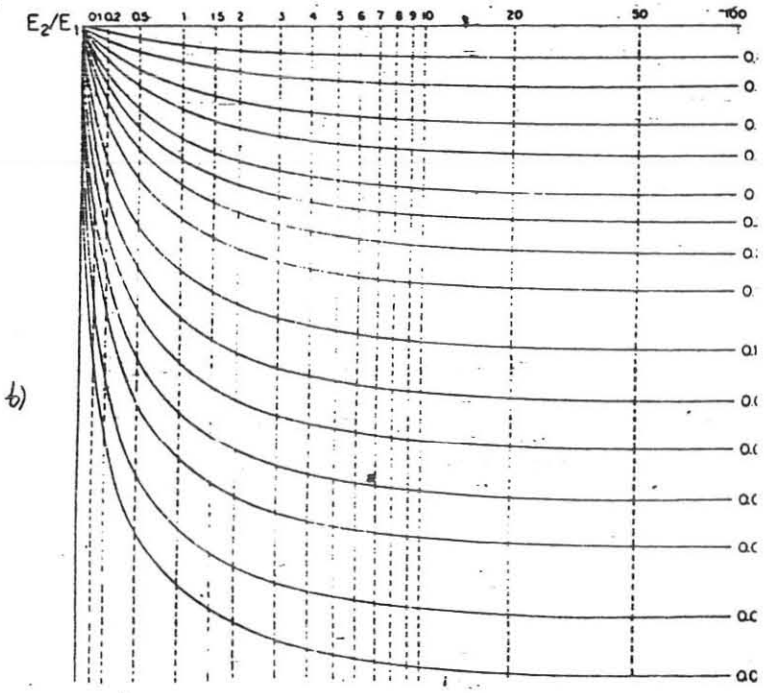

Fig(6)

ORELLANA- MO

6) Place OB onto SC and, while keeping the origin of SC along the trace IV and also keeping axes of both parallel, move OB until the e-f portion is best matched with one of the curves of the SC. Mark the origin of SC onto OB plot $O_5 = (h_{e5}, \rho_{e5})$ and read μ_5 of the matched SC curve so that $\rho_6 = \mu_5 \rho_{e5}$. In order to find the thickness of the fifth layer, put o_4 on the ordinate point with value μ_4 of the AC-K, while keeping axes parallel, and then read diagonally the value of the curve at which 0_5 lies. This gives ν_4 so that $h_5 = \nu_4 h_{e4}$.

b) Computer Aided (Modeling) Techniques

The manual procedure involves matching of the theoretically published curves with that of the field curves plotted on the same logarithmic scale as that of theoretical curves. This procedure is useful in the field situation for the depth investigation of the layer(s) in which we are interested for further studies using horizontal resistivity mapping . However, it is time consuming and not reliable.

On the contrary, the correct solution can be derived from VES curves in very short time by using a computer. Since 1973 various authors have published methods for automatic processing of VES data in which the computation of the layer parameters, are made by the computer. Of these different methods, at present the iterative methods are the most widely applied tool in the interpretation of resistivity sounding measurements.

In the iterative procedure the digital filtering procedure is used to calculate apparent resistivity at a series of points on the logarithmic scale for the assumed model; and this theoretical apparent resistivity value is compared with those obtained from the field measurements. The procedure works iteratively until the equation $(\rho)_{theoretical} - (\rho)_{observed} = 0$ holds.

The computer program for the iterative interpretation methods can handle horizontally-layered earth situations up to ten layers (including the substratum). The input to the program consists of the resistivities and thickness of the layers and the output consists of a series of plotted points, which then joined up to form the apparent resistivity versus electrode separation.

Briefly, the method consists of :

a) Assuming an initial model. This can be obtained from the manual procedures discussed above or from information such as borehole data, etc.

b) Obtaining, by means of the recurrence formula given in equation (10), the resistivity transform function for the assumed model.

c) Calculating the convolution of this resistivity transform with the known resistivity filter to obtain the theoretical apparent resistivity values.

d) Comparing the theoretical apparent resistivity values with that obtained from the field measurements.

If the agreement between the two sets of data is unsatisfactory, then the layer parameters are adjusted and then step (d) is repeated.

This procedure continues until a sufficient agreement between the model data and the field data is obtained or a set error limit is attained. Of course, at this stage of the interpretation we also incorporate into the resistivity section any information obtained from other geophysical and geological investigations.

2.4.2. Interpretation of Horizontal Profiling Data.

The interpretation of profiling data is qualitative, and the primary value of the data is to locate geologic discontinuities and structures such as faults, veins, dikes and buried stream channels.

To illustrate the theory, consider the case of concealed faults by tripole electrode configuration (or the half-Schlumberger Array) in which one electrode is removed to infinity. For practical reasons, one most often remove one of the current electrodes, usually B as shown in Fig.(7). It is AMN (c_1 p_1 p_2) that yield the Tripole Array.

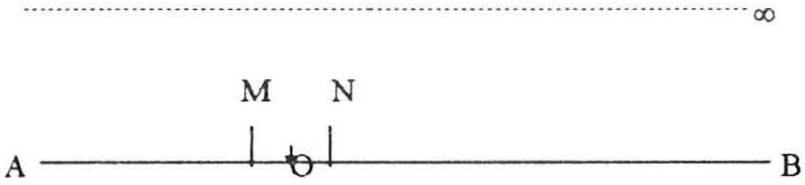

Fig.(7): The Half - Schlumberger Array

The potential difference between M and N is given by

$$\Delta V = (MN)\ E \qquad (22)$$

where E is the magnitude of the uniform electric field intensity between M and N (and this is true for small MN).

According to Ohm's law E is related to J, the magnitude of current density between M and N , by $E = \rho J$ where ρ is the resistivity in the vicinity of MN. Substituting this into equation (22) for E, gives

$$\Delta V = \rho J(MN) \qquad (23)$$

Hence, equation (19) becomes

$$\rho_a = G(MN)\frac{J\rho}{I} \qquad (24)$$

For a homogeneous isotropic media $\rho_a = \rho$, and $J = J_o$ is the current density in the homogeneous isotropic medium of resistivity ρ. The above equation for this medium then becomes

$$1 = G(MN)\frac{J_o}{I} \text{ or } G(MN) = \frac{I}{J_o}$$

Substituting this into equation (24) for $G(MN)$ one can express ρ_a in terms of J and J_o as

$$\rho_a = \rho\frac{J}{J_o} \qquad (25)$$

Any change in J due to concealed anomalies conductivity's cause, therefore, similar change in ρ_a , i.e., an increase in current density J beneath MN will result in an increase in apparent resistivity ρ_a , and vice versa. The change of ρ_a as the array crosses a fault can be assessed by assuming that the potential field at MN is caused by a single point current electrode, A , since the second current electrode, B, is far away from A.

The change of ρ_a across a steeply dipping fault for example, is shown in Fig.(8).

In the following it is assumed that the medium is homogeneous and isotropic with resistivity ρ_1 except for a small vertically standing low resistivity zone (a fault) of resistivity ρ_2 in the center.

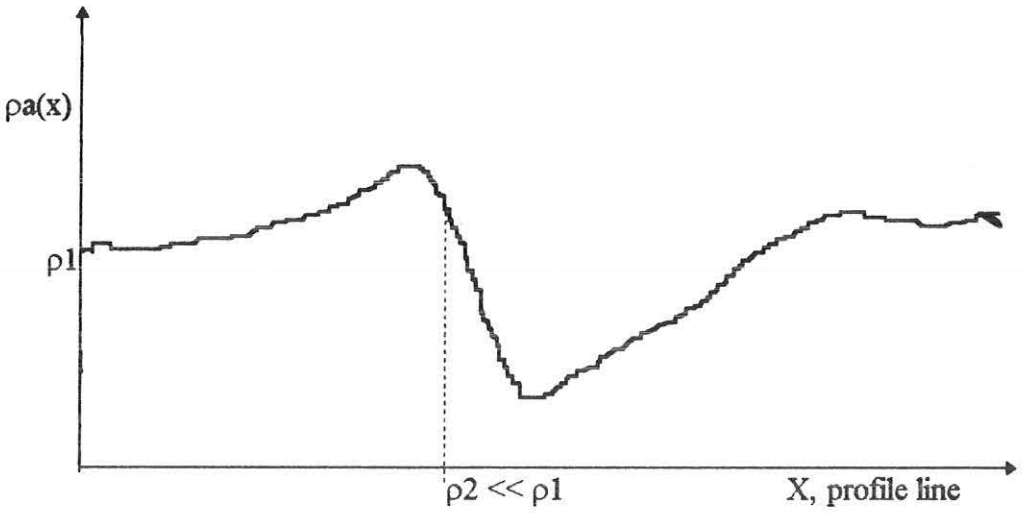

Fig.(8) : Schematic of ρa(x) over vertical fault when the resistivity on both sides of the fault is greater than the resistivity of the fault zone, ρ2<ρ1.

(1) If AMN is far away from the fault, then $J = J_o$ and hence equation (25) gives $\rho_a = \rho = \rho_1$, as indicated by the value of ρ_a on the far left of Fig. (8).

(2) If AMN approaches the fault from the LHS but both A and MN lying to the left of the electric field at MN the current will be distorted, since the current will tend to be "absorbed" by the fault zone, i.e., the current density J beneath MN increases and like wise ρ_a.

(3) When electrode A is on the LHS of the fault and MN on the RHS, the current density J will be greater in the fault zone but the current density J beneath MN will be reduced, i.e., ρ_a will decrease.

(4) When both A and MN lie on the RHS of the fault, J will increase until $J = J_o$ and likewise ρ_a increases until $\rho a = \rho = \rho 1$.

On the other hand, if the layer to the right of the fault has a resistivity $\rho 2 < \rho 1$, the curve of Fig. (8) will take a different form, a form as shown in Fig. (9), i.e., when both A and MN lie to the RHS of the fault, the apparent resistivity measured will not rise again but decreases and finally approaches the value ρ_2 .

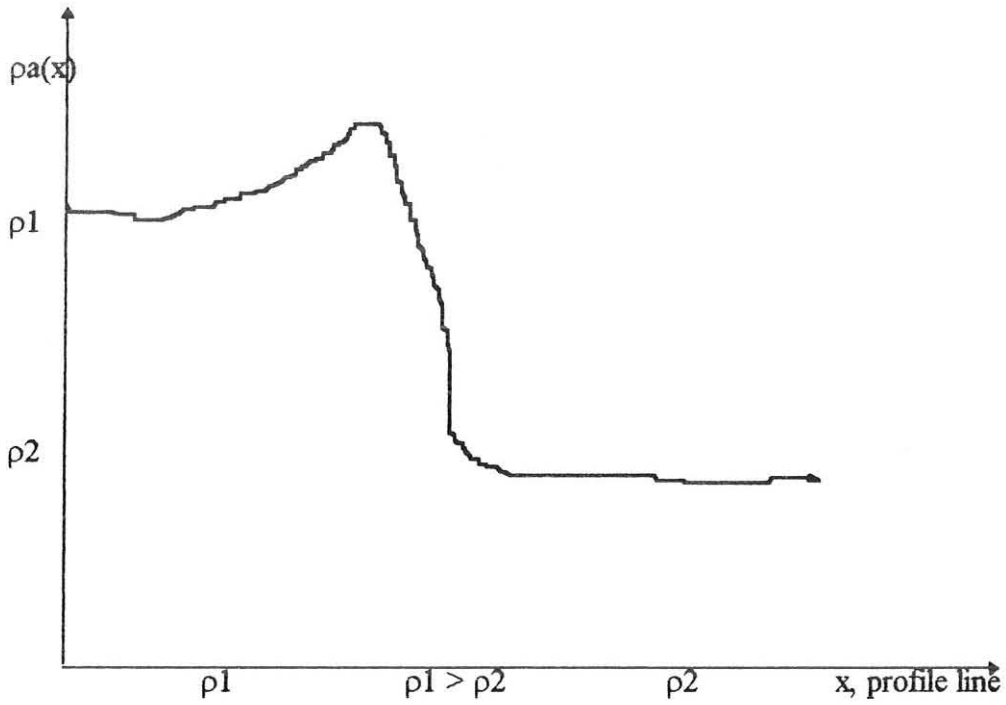

Fig .(9): Schematic of ρ_a over vertical fault when the resistivity is ρ_1 on the LHS of the fault and ρ_2 on the RHS of the fault such that $\rho_2 < \rho_1$.

CHAPTER III

Application of Resistivity Methods for Groundwater Exploration Around Chuko

3.1. Geophysical Investigations

3.1.1. Survey Layout and Summary of Statistics used

The following figure shows the survey layout, VES points and also the data points used for this thesis work. The twenty six sounding points are indicated by the symbol +, the two VES measurements taken around the borehole at Chuko town are indicated by BH and the resistivity profiling measurements are taken along the first five profiles with a station interval of 100m.

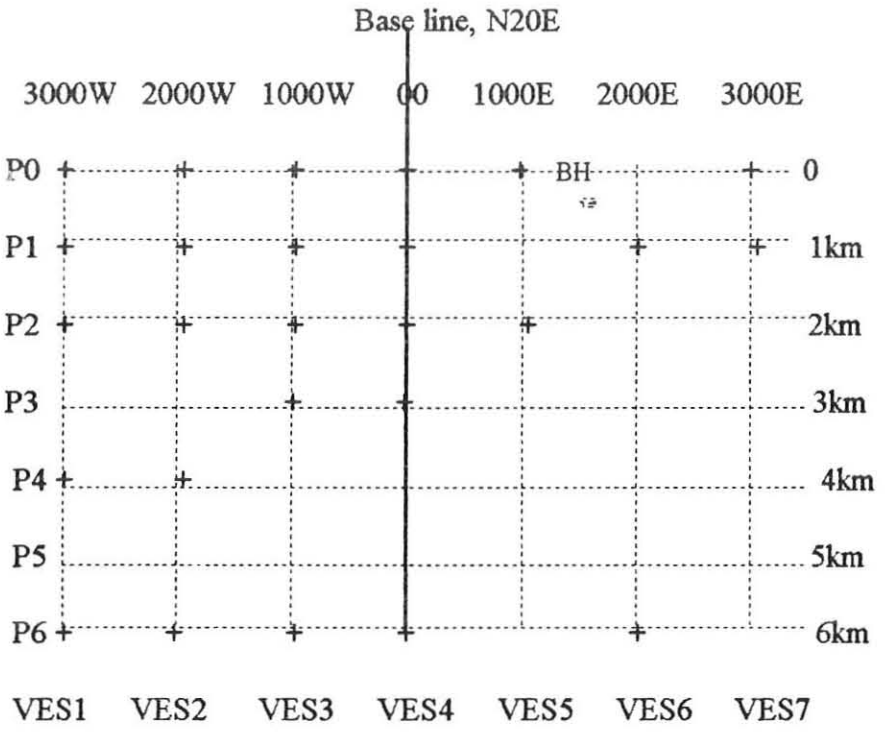

Fig.(10) : Survey Layout

3.1.2. Data Processing and Presentation of Results.

The resistivity profiling were taken along the first five profiles using the asymmetric three-pole array with AB/2 = 75m & MN/2 = 15m. The data were manually smoothed with the moving average window length equals five in order to remove the errors that arise mainly due to the instability of the measuring unit. The stacked section and contour maps of the smoothed resistivity profiling are given in Figures (11), (13) & (14).

The VES data were smoothed based on the theory which can be stated for the Schlumberger array as "the separation between M and N must approximate zero," so that the curve assume the tendency of that part for which MN is small; i.e., for the same AB/2, the value of the apparent resistivity for small MN/2 contributes more to the curve than that part of large MN/2. In order to account for this, the VES data are smoothed manually using the formula:

$$\rho_a\left(\frac{AB}{2}\right) = \frac{3}{4}\rho_a\left(\frac{AB}{2}, \text{small } \frac{MN}{2}\right) + \frac{1}{4}\rho_a\left(\frac{AB}{2}, \text{large } \frac{MN}{2}\right) \quad (26)$$

With the help of this formula the noisy outlier which is basically instrument effect and other factors can be removed.

The pseudoelectric sections given in Figures (15b), (16b), (17b) and (18a) and also the contour maps given in Figures (13) and (14) are prepared manually following the usual procedure. In other words by joining points with the same resistivity value.

The type curve map is produced in order to study the tectonic features of the survey area. The type curve map is prepared by putting identical type curves at the respective VES stations into one category (example of type curves HK, KH, QH, AK, HAK, QHAK, etc.). This is shown in Fig.(19).

In order to study the problems of principles of equivalence two VES curves: one at the borehole station in Chuko town and the other at profile P_o, station 1000E approximately 500m away from the borehole are interpreted with sets of different models as shown in Fig.(20) and (21).

In order to prepare geoelectrical sections the initial model is obtained from the curve matching procedures with the help of two-layer plus auxiliary point method. The final model is prepared using iterative procedures with the help of the RESIST software. These geoelectric section maps are given in Figures (15c), (16c), (17c) and (18b). However it was seen that since the initial model was carefully prepared, the final model is almost the same as that of the initial ones prepared manually on millimeter paper.

The stacked section of the graphic plots of the smoothed apparent resistivity curves with moving average window length equals five is shown in Fig.(11).

Across profile Po four resistivity sections are observed: constant low resistivity value 10-25 ohm-m in the region from 3000W to 400W, linearly increasing apparent resistivity section from 500W to 1300E, constant high resistivity value 70-85 ohm-m from 1400E to 2000E, and finally linearly decreasing apparent resistivity section from 2100E to 3000E. The constant resistivity values are associated with the mass or content of rocks where the fluctuations of the values around this constant indicates the degree of fracturing of rocks; and the linear increase or decrease of apparent resistivity for sufficiently large distance are the indications of geologic structures such as faults, joints, contacts, etc.

Hence as shown across this profile the left part is characterized by low resistivity value with less resistivity variation and this is due to the high clay content or due to the clay mass. The linear increase in the middle part and the linear decrease at the end of the right hand side are due to the assumed faults. In between these two faults constant but fluctuating resistivity values are observed and these are associated with fractured rocks promising for ground water occurrence.

It follows from the above discussion that a given apparent resistivity section can be described by the linear function of the form $\rho_a(x) = ax + b$ where the slope a has the dimension of resistance (ohm), the linear variable x has the dimension of length (meter) and the intercept b has the dimension of resistivity (ohm-meter).

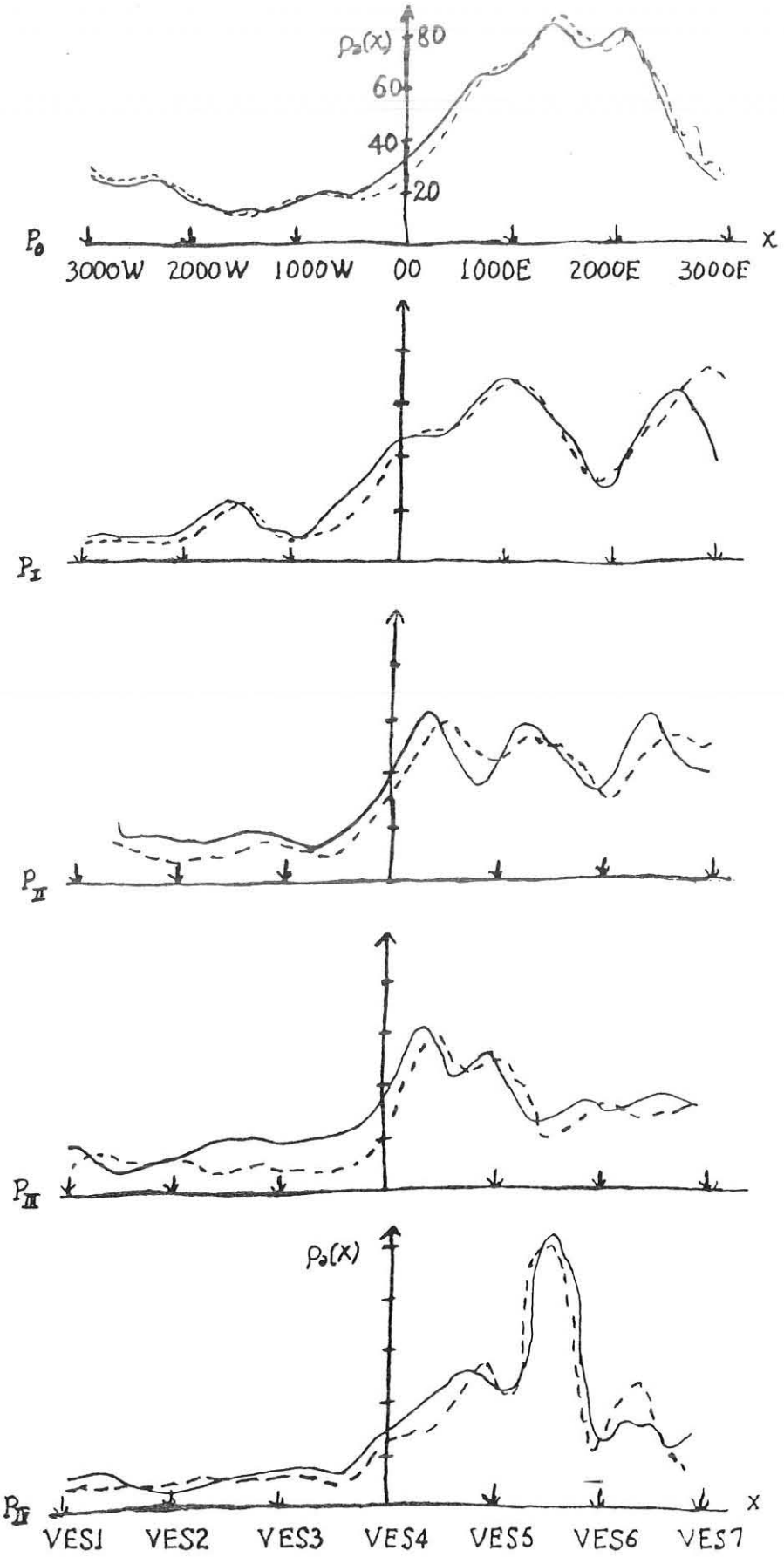

Fig(11) : stacked section

Apparent resistivity curves for asymmetric array
(moving average window length equals five)
scale : 1 : 67000

By using least squares approximation method the values of a and b are given for profile P_0 as follows: for 3000W-400W a = _0.0295 ohm and b = 22.2 ohm-m, for 500W-1300W a = 3.85 ohm and b = _ 82 ohm-m, for 1400E-2000E a = _0.0138 ohm and b = 78.9 ohm-m, and for 2000E-3000E a= _6.5 ohm and b=405 ohm-m.

Now in order to acquire the meanings of a and b consider the fault zone with left hand side material of the fault has resistivity ρ_1 up to x_1 distance away from some reference point and the right hand side material has resistivity ρ_2 starting from x_2 distance onwards as shown in the figure below.

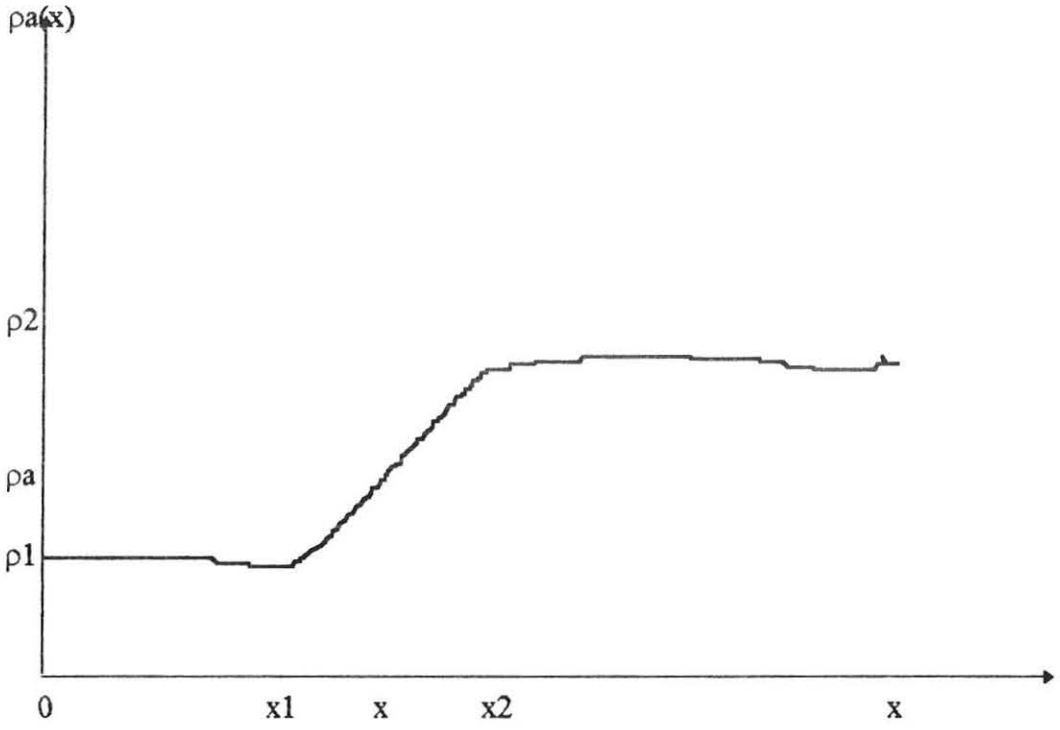

Fig.(12): Theoretical model of apparent resistivity versus horizontal distance at a given horizon having geologically meaning thickness.

$$Slope = a = \frac{\rho_a(x) - \rho_1}{x - x_1}$$

From which we get $\rho_a(x) = ax + \rho_1 - ax_1$

But $$a = \frac{\rho_2 - \rho_1}{x_2 - x_1}$$

so that $$\rho_a(x) = ax + \rho_1 - \left(\frac{\rho_2 - \rho_1}{x_2 - x_1}\right)x_1$$

or $$\rho_a(x) = ax + b$$

where $$b = \frac{\rho_1 x_2 - \rho_2 x_1}{x_2 - x_1}$$

For the case when $\rho_1 = \rho_2$ we have a = 0, b = $\rho_1 = \rho_2$ and also $\rho_a(x) = \rho_1 = \rho_2$. And for the case when ρ_1 and ρ_2 are different both a and b are different from zero. Hence a describes the fault zone and b describes the relationship between the materials on the sides of fault zone.

The region between 1400E and 2000E can be divided into two zones: for 1400E-1700E a_1 = _3.92 ohm and b = 218.86 ohm-m, and for 1800E-2000E a_2 = 4.0 ohm and b = _141.5 ohm-m. But $a_1 + a_2 = a_{net} = 0.08$ ohm $\cong 0$ and $b_1 + b_2 = b_{net} = 77.36$ ohm-m. Hence a_{net} and b_{net} have identical values as the one's we get by directly applying least squares approximation for the whole region 1400E-2000E. The addition of slopes of minor faults a_1 and a_2 approximates the value zero which is that of the fault in the region. The reason is that because least squares approximation holds, the fluctuations of resistivity values around the constant value can be removed so that the apparent resistivity assumes the true resistivity value 77 ohm-m.

Since there is no fault in this region the minor faults can be associated with simple fracturing of rocks in the region , and the addition of slopes can be imagined as the arrangements of these minor faults as resistors in series connection.

The net resistance is associated with the dip angle of the fault say θ and the relationship between them is given by $\tan\theta = a_{net}$ so that since there is no fault in the region between 1400E and 2000E $a = a_{net} = 0$ and hence $\tan\theta = 0$ or $\theta = 0$. For the region 3000W-400W the dip angle is given by $\theta = \tan^{-1}(-0.295) = 16.4^0$, for 500W-1300E $\theta = \tan^{-1}(3.85) = 75^0$, and for 2100E-3000E $\theta = \tan^{-1}(-6.5) = 81^0$.

Across profile P_I , as shown in Fig.(11), low resistivity value 10-20 ohm-m with less fluctuation in the values is observed in the region 3000W-1000W and this is due to clay mass. In between 1000W and 1000E the apparent resistivity value is linearly increasing due to the fault. In the region 1000E-3000E, the resistivity is highly varying and these high resistivity variation yielded sets of line segments with their corresponding slopes joined to one another. When least squares approximation is applied these line segments which are associated with minor faults can be removed and the apparent resistivity assumes the constant mean value equals 50 ohm-m which is fractured rocks with fresh water in it.

Since the apparent resistivity in this case is horizontal line the slope zero and this must be identical with the sum of the slopes of the line segments associated with the minor faults. This is true because the minor faults can be imagined as resistors in series. The dip angle of the fault around the base line is approximately equals 75^0.

The graphic plot across P_{II} , as shown in Fig.(11), shows low resistivity value 15 ohm-m with no fluctuation in the region 2600W- 500W; and this is due to the clay dominance. The apparent resistivity in the middle part is linearly increasing due to fault. In the region between 500E and 3000E high resistivity fluctuation is observed but it has the tendency of assuming horizontal line; and applying least squares approximation the resistivity of this region assumes the value 55 ohm-m so that this is fractured sand with fresh water. Though the minor slopes are not zero, the sum of slopes of this region is zero; and this situation suitably describes fracturing of the rocks. However in the left part 2600W-500W there are no minor slopes and hence the net slope is zero so that this is associated with the rock which is not fractured and it is uniform. The dip angle of the fault around the base line is nearly equals to 80^0.

Across profile P_{III} , as shown in Fig.(11), low resistivity value 10-20 ohm-m with no fluctuation is observed in the region 3000W-300W and this is due to the clay material. From 300W to 300E apparent resistivity is linearly increasing due to fault, and then apparent resistivity is decreasing with fluctuation at some points around 500E, and this fluctuation is due to fracturing of rocks .

The resistivity maintains this uniform value nearly equals 35 ohm-m with less fluctuation in the region 1500E-3000E, and this is sand mass. The dip angle the fault around the base line is equal to 85^0.

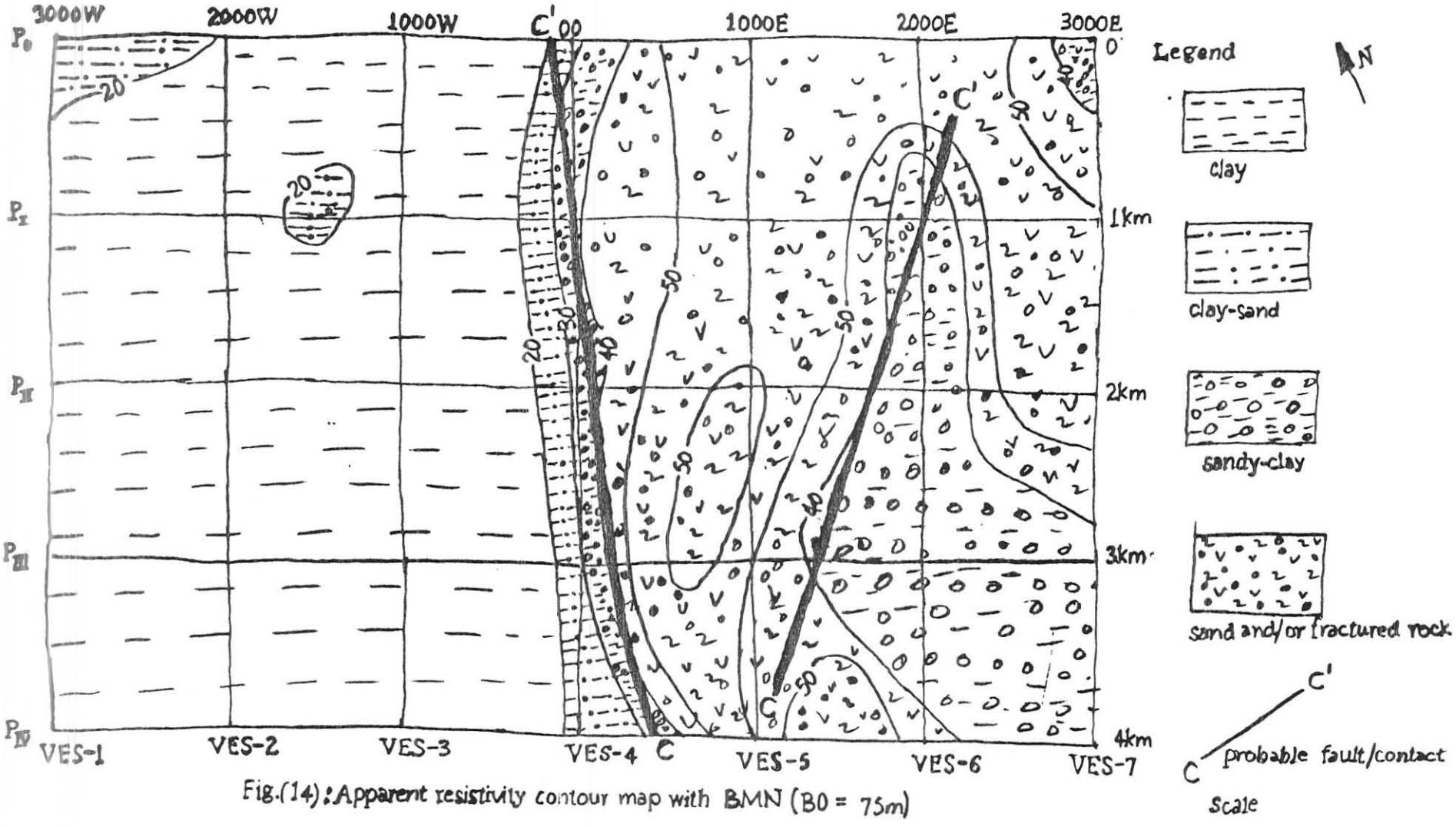

Fig.(14): Apparent resistivity contour map with BMN (B0 = 75m)

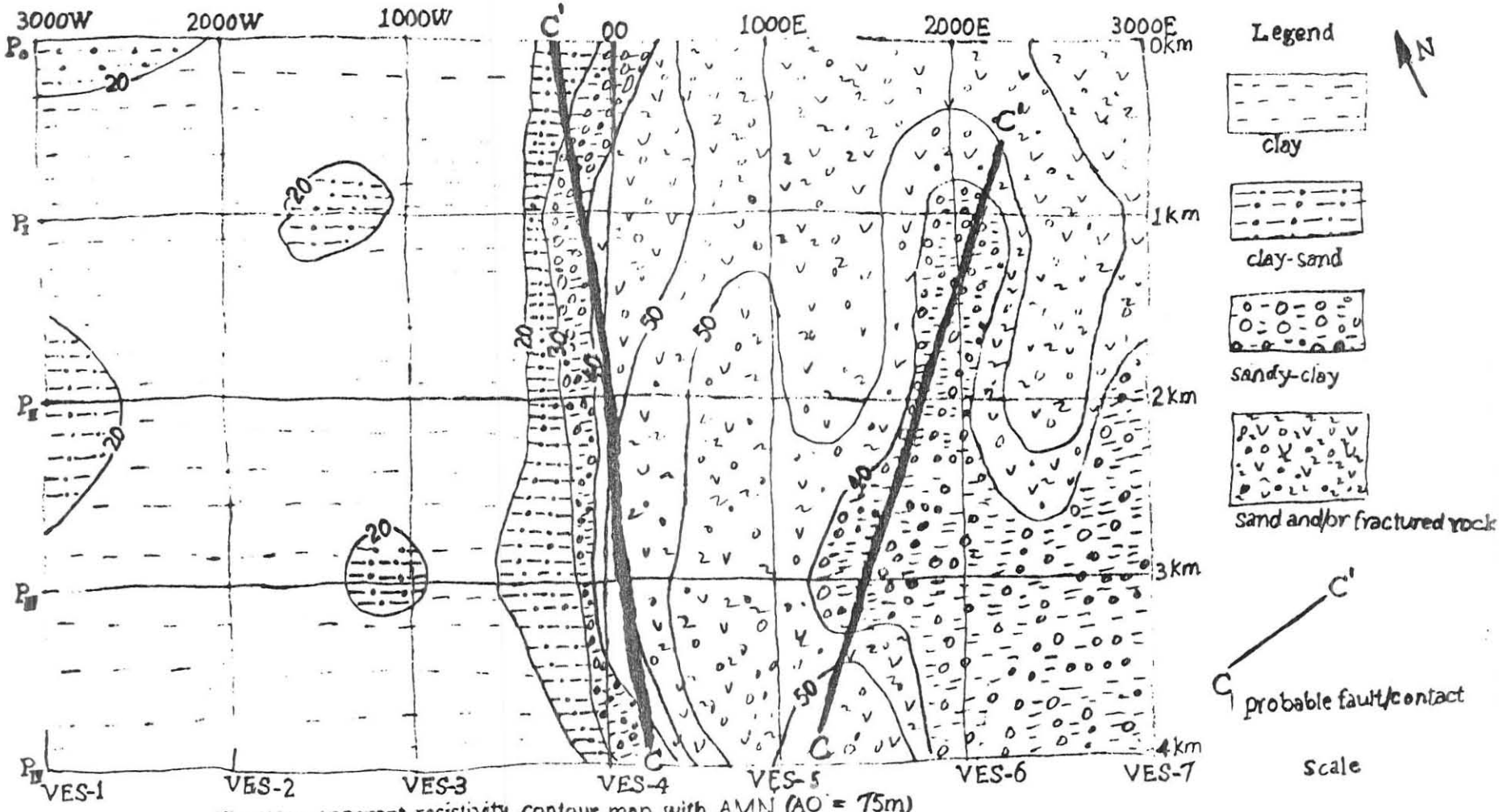

Fig.(13): Apparent resistivity contour map with AMN (AO = 75m)

Across profile P_{IV} , as shown in Fig.(11), the left hand side 3000W-500W has very low resistivity value 10 ohm-m which is highly clay massive zone. In between 500W-800E due to the fault the apparent resistivity is linearly increasing. The dip angle of the fault around the base line is approximately equals 72^0.

In the contour maps of Figures(13) and (14) low resistive zone is observed from the left up to the base line, uniform increment around the base line is observed due to the lineament structures such as faults and the right hand side of the base line has sufficiently large resistivity and the resistivity in this region is highly varying due to the fracturing of rocks.

In general the left hand side clay, the middle part around the base line is fault zone and the right hand side is fractured rock which is promising for ground water production specifically for the first three profiles P_0 , P_I and P_{II} as shown in Figures (11), (13) and (14).

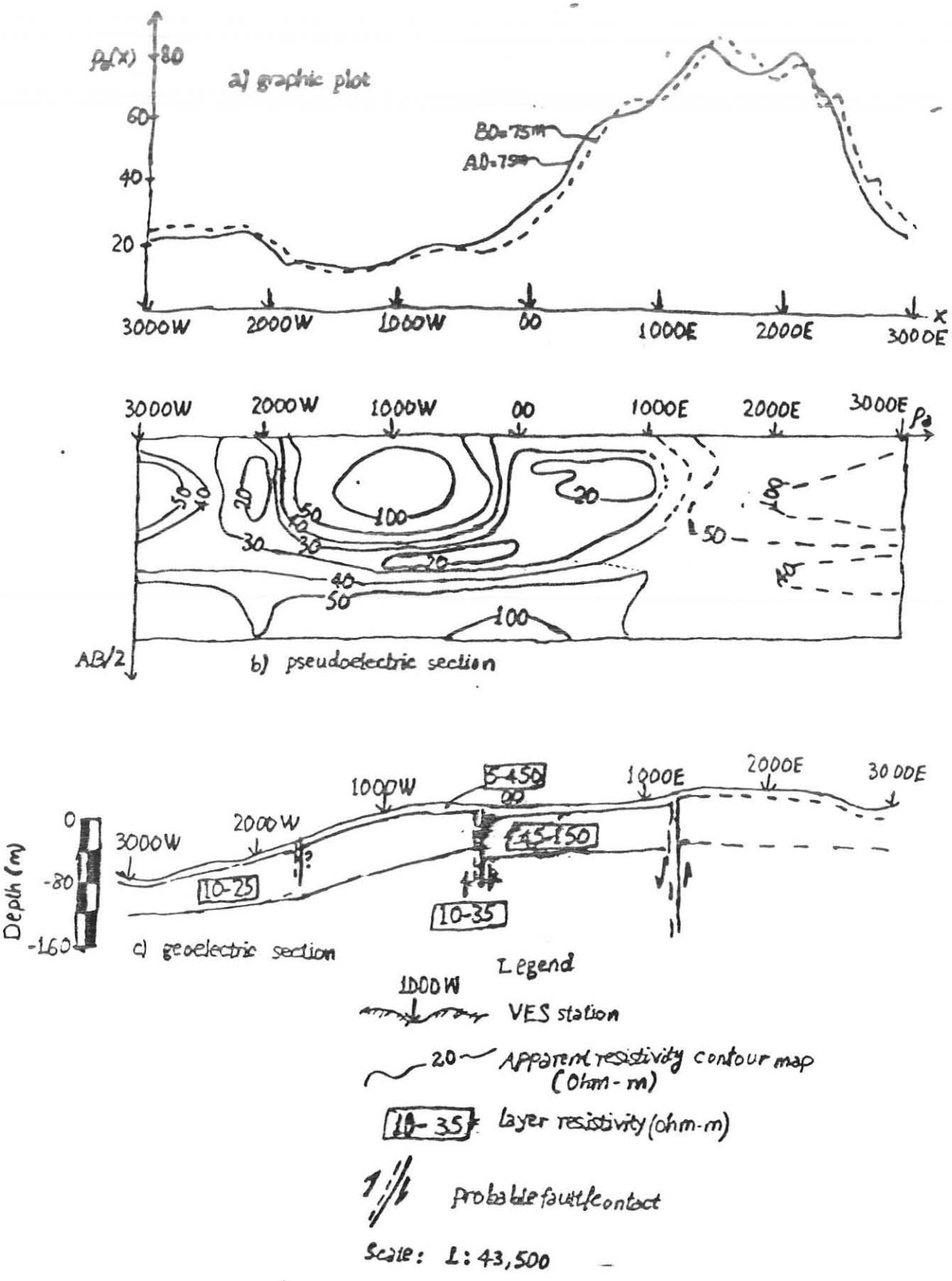

Fig.(15): Results of electrical resistivity survey along profile P_o

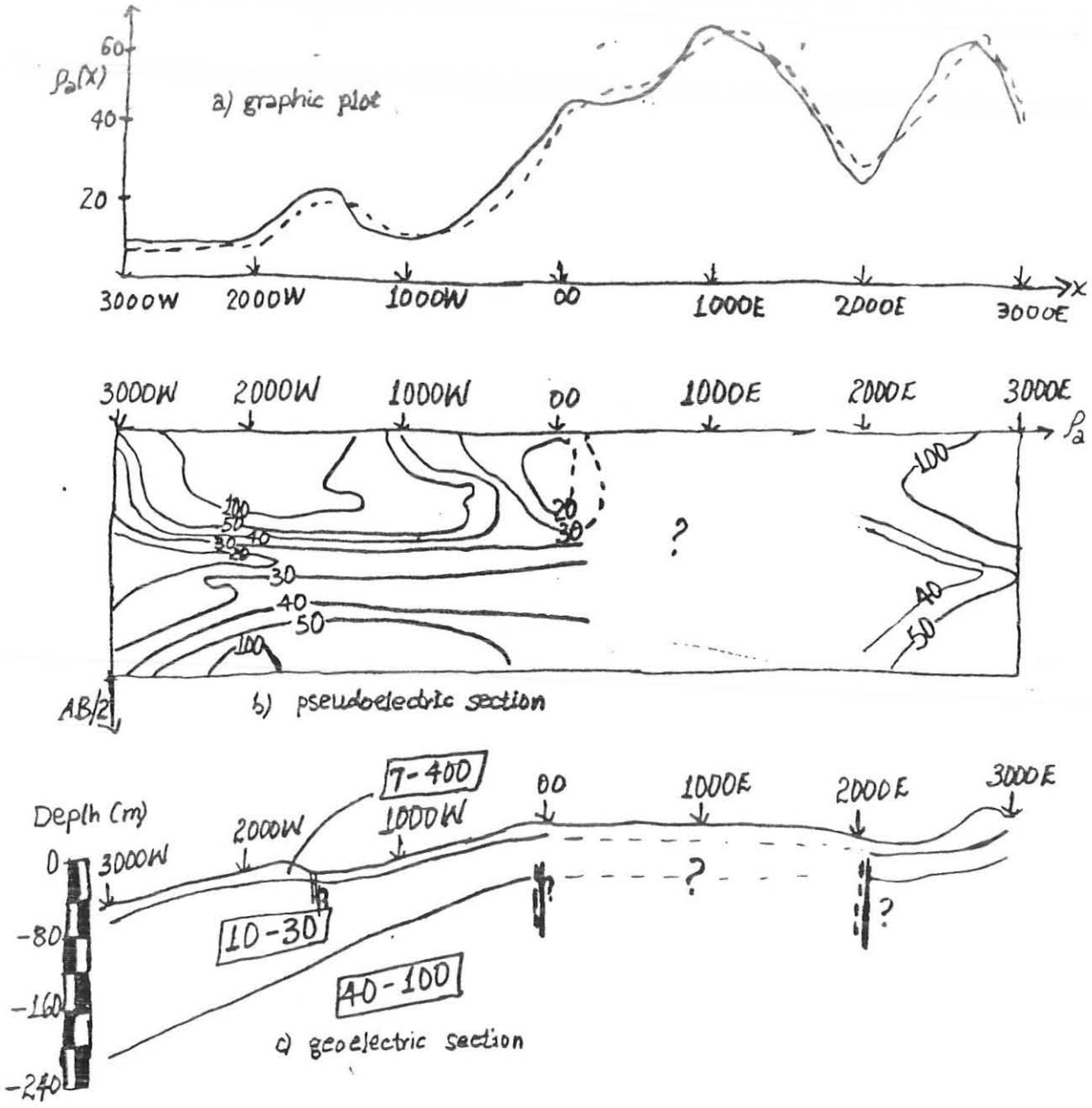

Fig(16): Results of electrical resistivity survey along Profile P_I

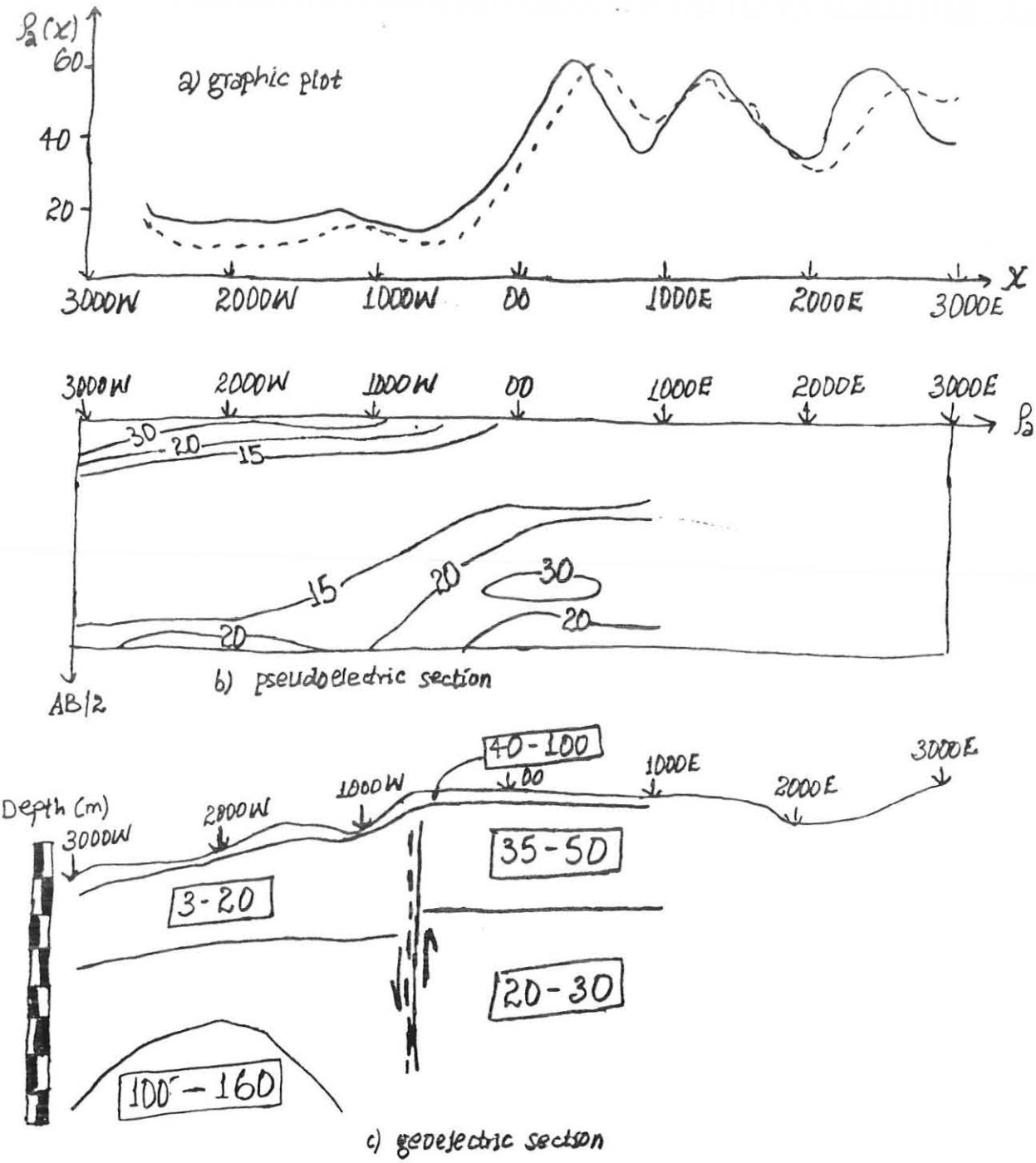

Fig(17): Results of electrical resistivity survey along Profile P_{II}

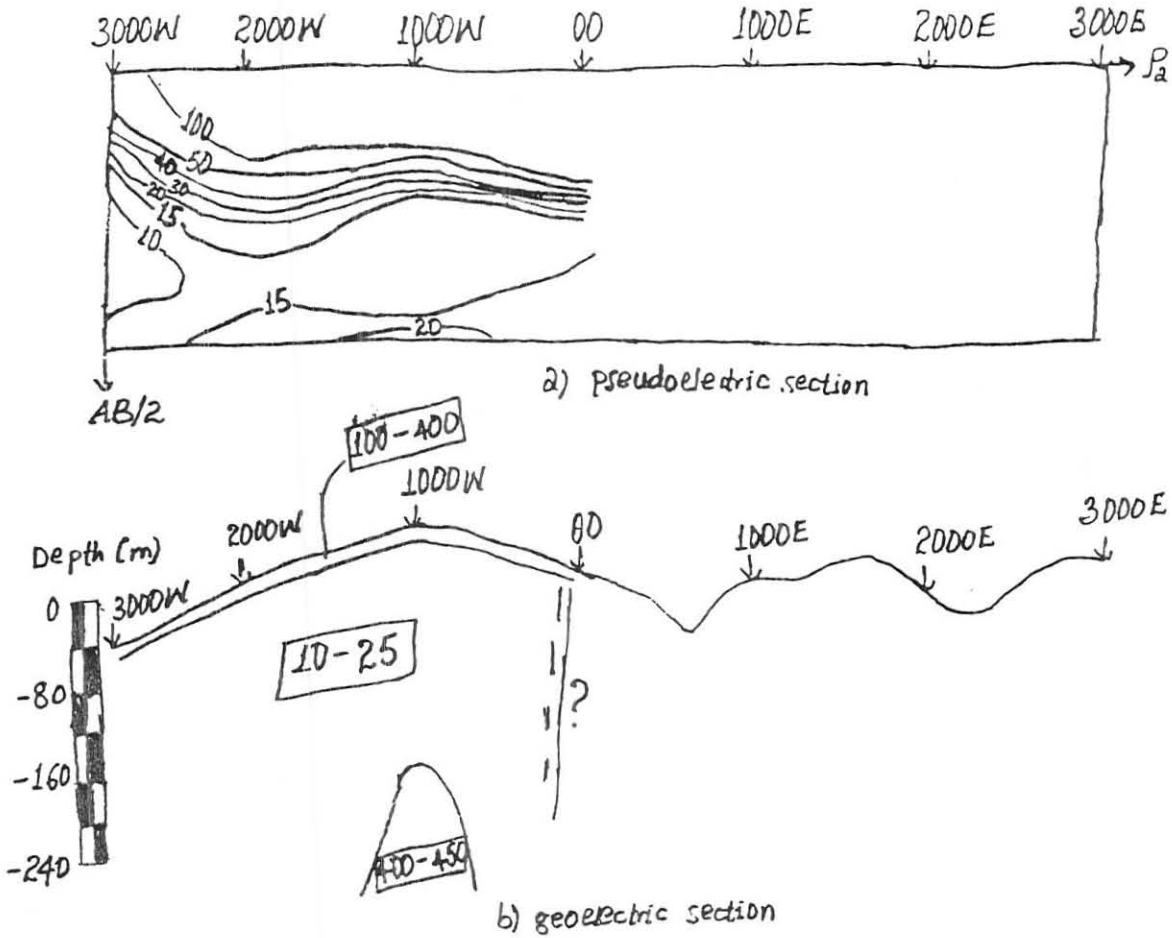

Fig(18): Results of electrical resistivity survey along Profile P_2

The geoelectric section of the subsurface beneath profile P_o , as shown in Fig.(15), can be interpreted as three-layer section. The top-layer has resistivity 5-450 ohm-m and its depth varies up to 5m. The great resistivity variation in the range of this overburden material is mainly due to the lithological differences. The second layer in the depth range 20-80m with resistivity 45-150 ohm-m seems to be composed of sand, gravely sand, fractured ignimbrites, etc. in the region 2000W-3000E; and it has resistivity 10-25 ohm-m in the left hand side which may be due to clay, ash, or clay-sand etc. The third layer has low resistivity value 10-35 ohm which is probably due to clay dominance.

The graphic plot analysis at the depth range 35-45m shows that the low resistivity (10-25 ohm-m) material with less fracturing is encountered in the region 3000W-500W which is due to clay influence. Apparent resistivity is linearly increasing in the region 500W-500E and this is probably due to the geologic structures such as lineaments, faults, joints, contacts, dykes, etc. The rock at this depth range in the region 500E-2500E has resistivity 60-90 ohm-m and good fracturing is observed.

From the pseudoelectric section for the AB/2 equals 66-100m, ρ_a is constant with value 30-40 ohm-m in the range 3000W-1000E, and this low resistivity value seems to be due to clay influence. And for 1000E-3000E the apparent resistivity variation is not clearly seen due to lock of VES data at 2000E.

However, we may observe from these three sections: graphic plot, pseudoelectric section & geoelectric section that the left hand side of the base line is composed of conductive formations such as clay, ash, etc. at the depth of about 35m and in general this region is not promising for groundwater yield. And at the depth range of 30-60m, the region in the right hand side of the base line along profile P_o seems favorable for ground water production.

As it is seen from the geoelectric section across profile P_I ,Fig.(160, three-layer case is observed. The top layer, which is overburden material, whose depth varies up to 4m has resistivity 7-400 ohm-m; and this wide range of resistivity variation is due to the lithological differences. The second layer whose depth varies largely, up to 250m in the west and 50m in the east, has resistivity 10-30 ohm-m; and these low resistivity formations are probably clay, clay-sand, ash, etc. The third layer has resistivity value from 40 to 100 ohm-m which may be due to formations such sand, sandy-clay, gravely sand, fractured ignimbrites, etc. & is probably a good water bearing horizon.

The pseudoelectric section shows that the apparent resistivity of the top part is highly varying horizontally as well as vertically showing the lithological differences among the rocks that form this layer. The middle part shows the low constant apparent resistivity value 20-30 ohm-m accounting the effect of clay dominance. The apparent resistivity of the lost part is also nearly constant but has large value from 40 to 50 ohm-m which may be due to existence of water.

However, we may observe from these three sections: graphic plot, pseudoelectric section & geoelectric section that the left hand side of the base line is composed of conductive formations such as clay, ash, etc. at the depth of about 35m and in general this region is not promising for groundwater yield. And at the depth range of 30-60m, the region in the right hand side of the base line along profile P_o seems favorable for ground water production.

As it is seen from the geoelectric section across profile P_I ,Fig.(160, three-layer case is observed. The top layer, which is overburden material, whose depth varies up to 4m has resistivity 7-400 ohm-m; and this wide range of resistivity variation is due to the lithological differences. The second layer whose depth varies largely, up to 250m in the west and 50m in the east, has resistivity 10-30 ohm-m; and these low resistivity formations are probably clay, clay-sand, ash, etc. The third layer has resistivity value from 40 to 100 ohm-m which may be due to formations such sand, sandy-clay, gravely sand, fractured ignimbrites, etc. & is probably a good water bearing horizon.

The pseudoelectric section shows that the apparent resistivity of the top part is highly varying horizontally as well as vertically showing the lithological differences among the rocks that form this layer. The middle part shows the low constant apparent resistivity value 20-30 ohm-m accounting the effect of clay dominance. The apparent resistivity of the lost part is also nearly constant but has large value from 40 to 50 ohm-m which may be due to existence of water.

The graphic plot shows that at the range of nearly 35m, the left hand side has low resistivity value 10-30 ohm-m due to the clay influence, the apparent resistivity is linearly increasing in the middle part which may be due to lineament structures; and the right hand side has high resistivity value 40-80 ohm-m and also the rock in this side seems to be fractured the behavior of which is manifested in the fluctuation of observed resistivity values.

Comparing the geoelectric section, pseudosection section, and the graphic plot we may conclude that the right hand side of the base line is good aquifer for the depth range of about 35-80 m.

From the geoelectric section across profile P_{II} , Fig.(17), three-layer case is observed. The top-layer has resistivity 40-100 ohm-m and depth up to 6m; and this overburden materials. The second layer whose depth is nearly goes up to 100m has resistivity value 3-20 ohm-m in the left hand side which may be due to clay influence and in the right hand side its value is 34-50 ohm-m which is due to sandy formations. The third layer has resistivity value less than 30 ohm-m which may be due to clay, ash, clay-sandy formations etc. A material of small lateral dimension with high resistivity value is observed at a depth of above 240m around 2000 W & this seems an intrusive material.

The pseudoelectric section shows in general low apparent resistivity value which tells us that the subsurface below profile P_{II} is highly dominated by clay for sufficiently large depth.

The graphic plot shows low resistivity value 10-20 ohm-m in the left hand side, Lineament structure in the middle and fractured material with large resistivity value 40-60 ohm-m in the right hand side at the depth of about 40m. These can be interpreted respectively as clay, fault zone, and fractured rocks.

Hence from these maps we can conclude that the right hand side of the base line is good water bearing at the depth of about 40m.

The geoelectric section across profile PVI, as shown in Fig.(18), shows two-layer section. The top-layer is overburden material with resistivity value greater than 100 ohm-m in the depth range up to 5m; and this large resistivity value is may be due to low humidity content. The second layer has resistivity value less than 25 ohm-m and this low resistivity value is due to clay or clay-sandy formation.

This situation is also clearly seen in the pseudoelectric section whose top part (for the measurements taken at small AB/2) has large apparent resistivity value greater than 100 ohm-m but the lower part (for the measurements taken at large AB/2) has low apparent resistivity value less than 20 ohm-m.

From these analysis it seems that this profile is not promising for ground water production for sufficiently large depths. However, further analysis using type-curve mapping, as shown in Fig.(19), shows that the region around the base line is promising for ground water yield. We may infer from these that free ground water may be available at shallower depths around the base line of this profile allowing one for hand- dug wells.

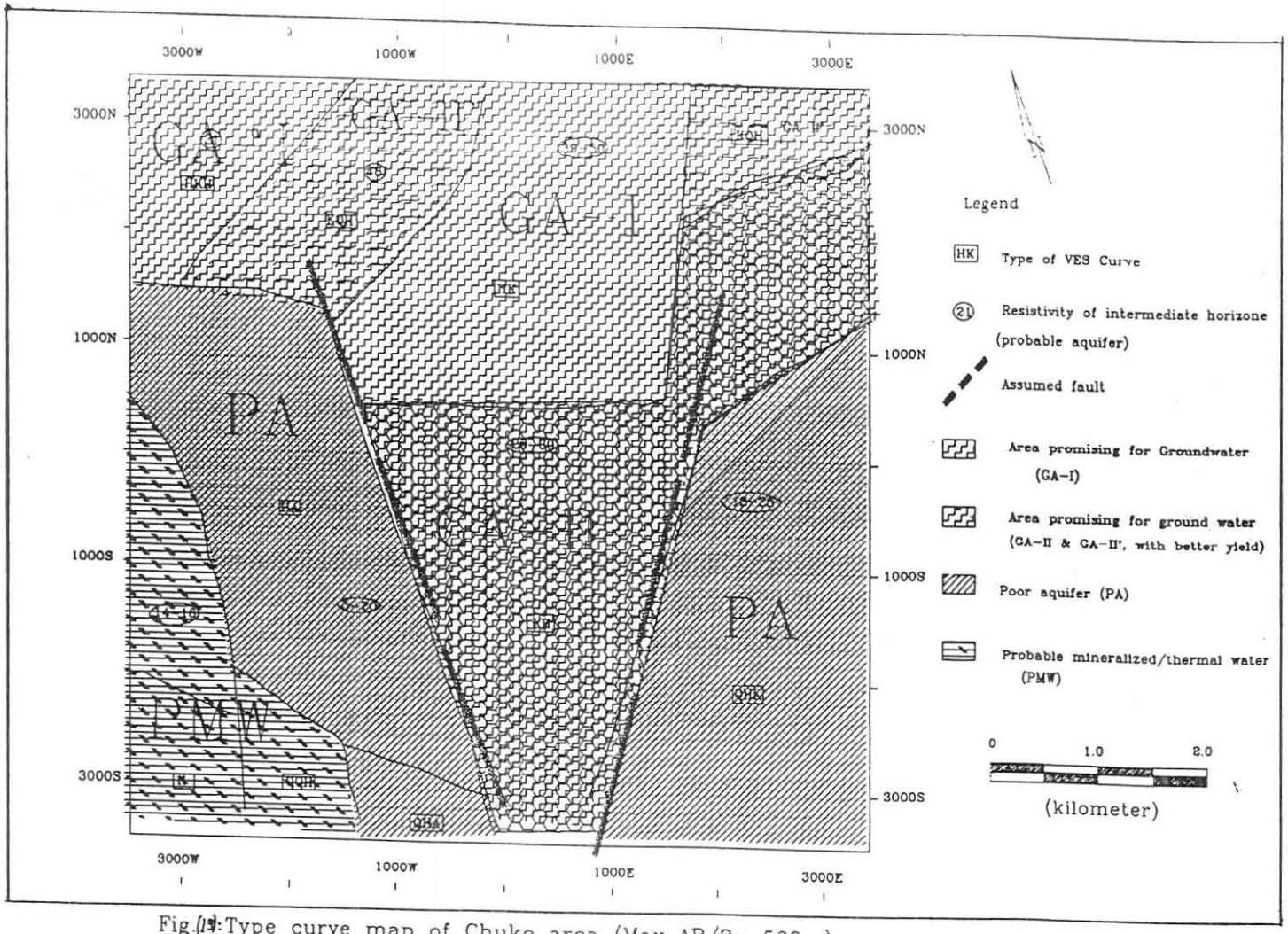

Fig.(1): Type curve map of Chuko area (Max AB/2= 500m)

The type curve map shown in Fig.(18) is produced by putting each type curve of the VES at their respective stations and then classifying the identical curves from the others by drawing an approximate boundary lines. These boundary lines are the representations of the plane separating zones and hence denotes the assumed structures.

The faults discriminated by using these boundary lines are as shown in the Figure (19). From these faults two zones are observed : the zone in between these two faults is characterized by the HK-type curve with the upper part having resistivty values in the range 30-50 ohm-m and the lower part having resistivity values in the range 40-100 ohm-m for the water bearing horizon. Hence this region is promising for ground water with better yield.

The far left side of the region between the faults is characterized by HA-type curve. The resistivity value of the subsurface in this region is 3-20 ohm-m. The right side of the region between the faults is characterized by QHK-type curve with the resistivity value for the region is 3-26 ohm-m. However, the upper part of both of these regions (near 3000N, and 3000W and 3000E) are characterized by KQH and HKH- type curves and the resistivity value of the layer that seems water bearing is 20-40 ohm-m. Though both of these regions seem promising for ground water yield in the upper parts, they are in general zones of poor aquifer.

The bottom of the left end side is characterized by QQH- type curve with resistivity value of the thick layer encountered is 14-16 ohm-m and these seem probable mineralized or thermal water.

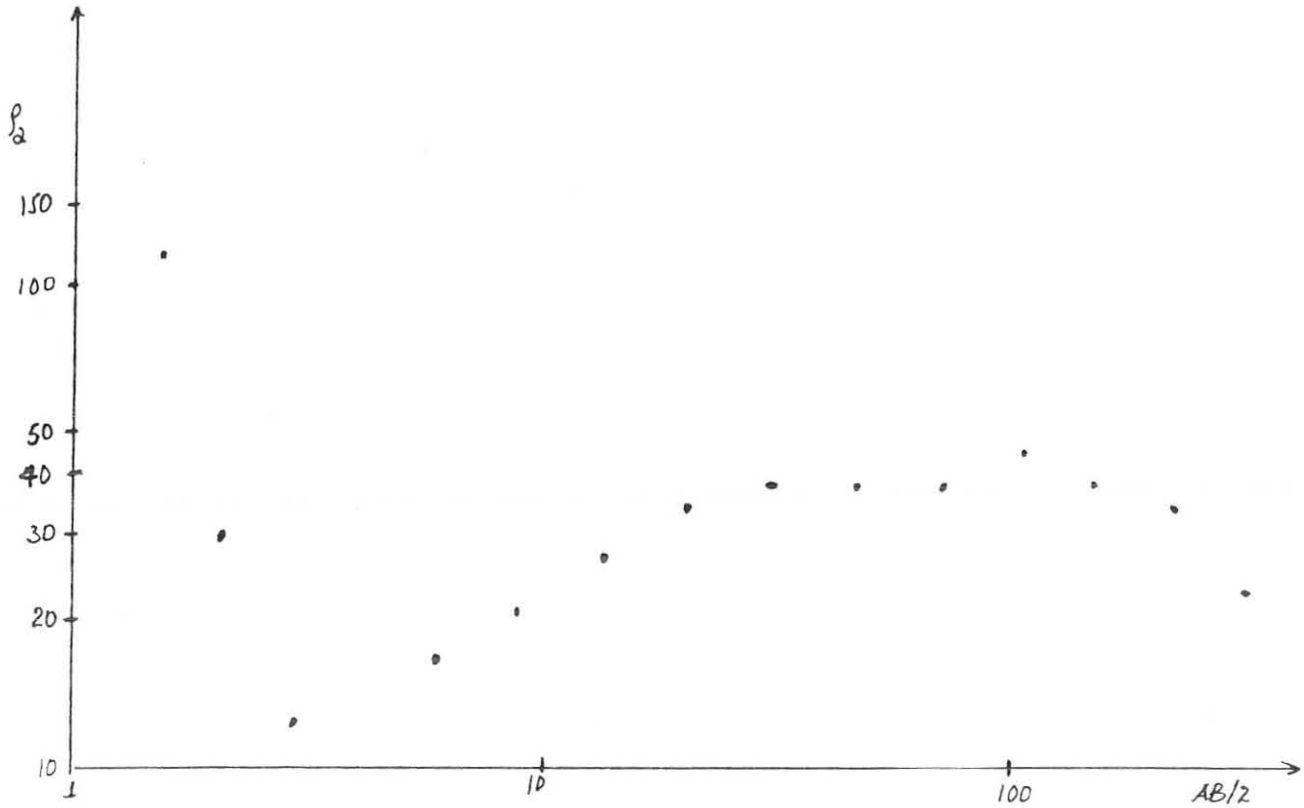

4-layer model : $\rho_1 = 634$ $\rho_2 = 8$ $\rho_3 = 54.7$ $\rho_4 = 17.5$
$h_1 = 0.5$ $h_2 = 2.5$ $h_3 = 107.2$

5-layer model : $\rho_1 = 694.8$ $\rho_2 = 7.4$ $\rho_3 = 55$ $\rho_4 = 50$ $\rho_5 = 17.1$
$h_1 = 0.5$ $h_2 = 2.2$ $h_3 = 8.3$ $h_4 = 115$

6-layer model : $\rho_1 = 621$ $\rho_2 = 6.4$ $\rho_3 = 55$ $\rho_4 = 50$ $\rho_5 = 51.3$ $\rho_6 = 15.3$
$h_1 = 0.5$ $h_2 = 1.9$ $h_3 = 10$ $h_4 = 20.2$ $h_5 = 99.1$

Fig.(20) : Interpretations of VES curve at the borehole in Chuko town for the station parallel to the profile.

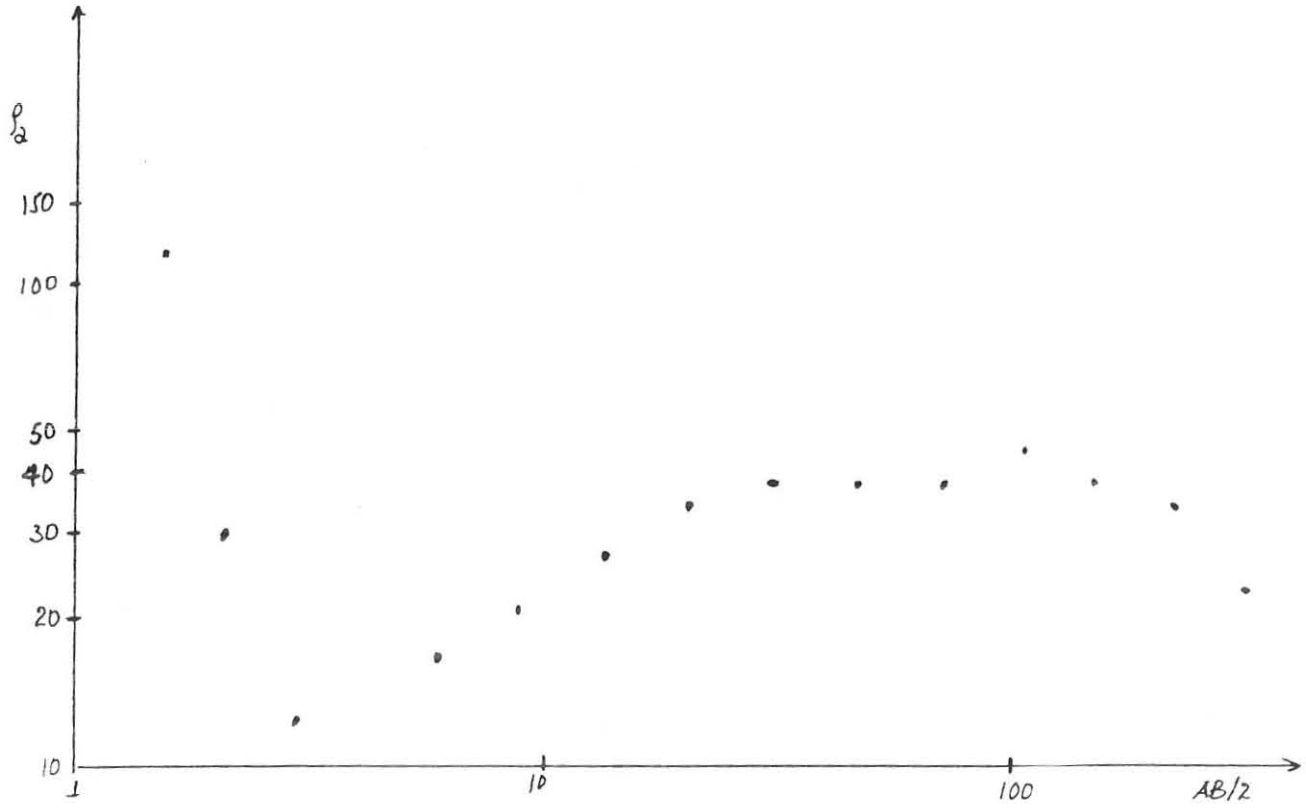

4-layer model : $\rho_1 = 634$ $\rho_2 = 8$ $\rho_3 = 54.7$ $\rho_4 = 17.5$
$h_1 = 0.5$ $h_2 = 2.5$ $h_3 = 107.2$

5-layer model : $\rho_1 = 694.8$ $\rho_2 = 7.4$ $\rho_3 = 55$ $\rho_4 = 50$ $\rho_5 = 17.1$
$h_1 = 0.5$ $h_2 = 2.2$ $h_3 = 8.3$ $h_4 = 115$

6-layer model : $\rho_1 = 621$ $\rho_2 = 6.4$ $\rho_3 = 55$ $\rho_4 = 50$ $\rho_5 = 51.3$ $\rho_6 = 15.3$
$h_1 = 0.5$ $h_2 = 1.9$ $h_3 = 10$ $h_4 = 20.2$ $h_5 = 99.1$

Fig.(20) : Interpretations of VES curve at the borehole in Chuko town for the station parallel to the profile.

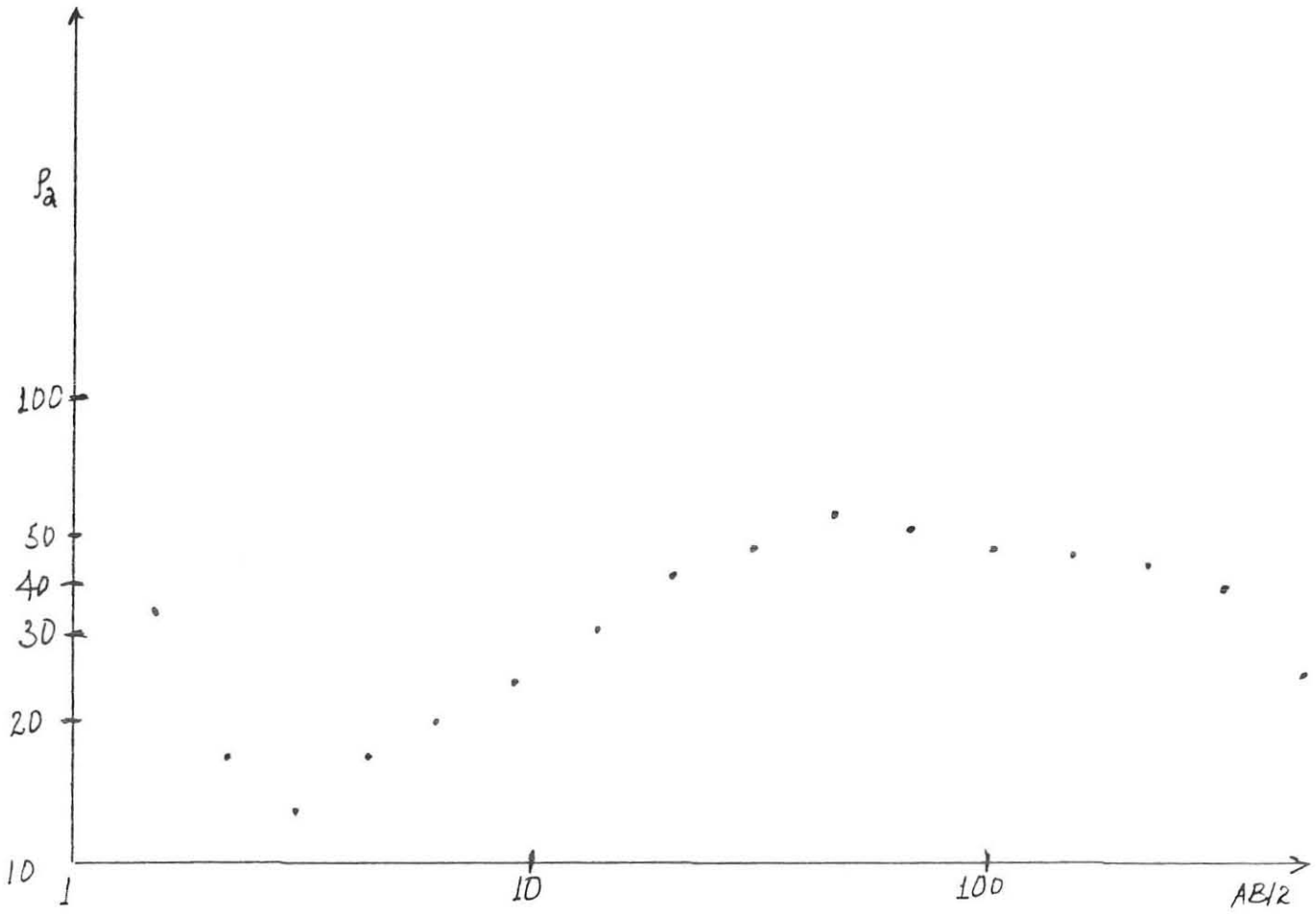

5-layer model : $\rho_1 = 148.7$ $\rho_2 = 6.3$ $\rho_3 = 60.2$ $\rho_4 = 46.3$ $\rho_5 = 7.7$
$h_1 = 0.5$ $h_2 = 1.3$ $h_3 = 30.3$ $h_4 = 204.7$

6-layer model : $\rho_1 = 142.9$ $\rho_2 = 4.7$ $\rho_3 = 78.6$ $\rho_4 = 60.1$ $\rho_5 = 46.3$ $\rho_6 = 5.7$
$h_1 = 0.5$ $h_2 = 1.1$ $h_3 = 7.9$ $h_4 = 13.4$ $h_5 = 225.1$

Fig.(21) : Interpretations of VES curve at profile P_0 , station 1000E, approximately 500m away from the borehole at Chuko town.

A selected two different VES curves, one of which has been conducted at the borehole and the other near the borhole (nearly 500m away from boreholes) along profile P_o, are interpreted with different models so as to analyze the influences of the principles of equivalence and to develop the possible ways to manage and handle these problems. Sets of different models of these curves are shown in Figures (20) and (21).

According to Slichter (1933) there is one-to-one relationship between the apparent resistivity of a VES curve and the thickness and the resistivity of the individual layers in a horizontally stratified ground. But there is a random distribution of every measured apparent resistivity value in a VES curve & the one-to-one relationship holds in theory. The main causes of this random distribution of apparent resistivity values are the geological, physical and experimental influences; but the geological effects are much greater than the physical or experimental ones together. Koefoed (1969a&b, 1979) has shown that the principle of equivalence is only a result of natural circumstances & not one of theory. And the causes this problem are the too low or too high values of transverse resistance or longitudinal conductance.

A VES curve at the borehole station surveyed parallel to the borehole station surveyed parallel to the profile, as shown in Fig. (20), can be interpreted with three different models, each representing a normal geological sequence a 4-layer, a 5-layer and a 6-layer model.

The other VES curve as shown in Fig. (21) can be interpreted with two different models, both representing a normal geological sequence a 5-layer and a 6-layer model.

The three different models of the borehole line curve have the following in common: a thin high resistive formation resistivity about 60 ohm-m & a relatively thick very low resistive of about 10 ohm-m form the top layer; a sequence of aquifers of varying number; and a bottom layer (with infinite thickness) of low resistivity about 15 ohm-m. The two models of the other curve have the following in common: a thin resistive formation with resistivity of about 125 ohm-m and a relatively thick formation of resistivity about 6 ohm-m form the top layer; a sequence of aquifers of varying number; and a bottom layer (infinite thickness) of low resistivity of about 8 ohm-m.

Hence it can be seen all three models have a similar general structure and that the only parts where differences occur are aquifers with the very low values of longitudinal conductance. Similar analysis of the VES curve from profile P_o nearly 500m away from the borehole at Chuko led to the same conclusion that the two models have a similar general structure but the only parts where differences occur are aquifers. Thus in both these differences alone are responsible for the variations in the interpretations of the curves.

For this particular survey area we may say that in the geoelectrical sounding using Schlumberger array for groundwater exploration, assuming horizontal stratification and other factors being remain constant, the main causes of the principle of equivalence is the differences in aquifers.

Therefore, the VES curve provides information about the general arrangement of the strata: about the top layer, the bottom layer, and possible strata in between. The information about the general structure can be derived from the geoelectrical sounding curve itself without any external information. The information regarding lithologic composition along with the layer parameters (thickness and resistivity) can be obtained from the combined interpretation of VES and geologic data. In other words the VES curves yield fine structure (or specific arrangement of strata) when incorporated with external geological information's . Hence, in the above examples the geological concept is necessary for the middle part of the general arrangement.

3.1.3. Discussion of Results

There are two main situations for which a geological concept must be developed for the interpretation of geoelectrical sounding curve. The first is when external information already exists for the area to be prospected. These information, which can be well descriptions, logs, maps, or any other data which cannot be derived from the geoelectrical sounding curve, is the basis for the development of a geological concept.

The second condition is the one were there is no information at all about the area; but geoelectrics are the first method to be used for exploring an area. If no external information is available for the interpretation of a geoelectrical sounding curve, the acceptable result which can be obtained from a sounding curve alone is a model. However, such practices results in different equivalent possibilities for interpreting a single geoelectrical sounding curve so that different models are possible and hence one can not decide a unique model for the given VES curve. This is referred to as principle of Equivalence.

From the hydrogeological point of view, since the electrical conductivity is mainly dependent on the groundwater chemistry; and the rock matrix has only a very small influence, one can fix the resistivity value for an aquifer over a large area. As long as the groundwater is chemically homogeneous over the area of interest, there is no reason not to consider it constant. Certainly, there are changes in the conductivity of an aquifer, but they can't be identified due to the restricted resolution of the geoelectrical instruments.

Now suppose that the resistivity value for an aquifer is known from external information's so that one can fix it at one value for the different models of a given VES curve. From the information's of the borehole at Chuko town the resistivity of aquifer is nearly in between 55 and 60 ohm-m. Hence from the hydrogeological point of view the resistivity value of the aquifer around Chuko can be fixed at one of the values in this range.

As it can be observed from the final results of inversion that when the resistivity value of aquifer is fixed at 55 ohm-m the three different models of the borehole VES curve, all the resistivity value of the layers bearing water which initially seems different layers, assume the value nearly equals to 55 ohm-m; and the depth range of aquifer is nearly identical in all different models (3m-100m). Similarly the same operation in the two different models of the VES curve from profile P_o give the resistivity values for all aquifers tending or converging to 60 Ohm-m ; and the same depth range for aquifer horizon. From these we may conclude that for the interpretation of VES curves of Chuko area, only the resistivity value of the aquifer is important but the number of layers is of negligible importance. Therefore, when interpreting VES curves for groundwater exploitation, if the cause of equivalence problem is aquifer, one can fix a known resistivity value for the aquifer than to estimate a new one for each model and then can reduce the effects of the principle of equivalence.

In general, we may conclude that the problem of the principle of equivalence does not alter very much in the interpretation of VES for the ground water exploration if aquifer resistivity is known from external information and the cause of the equivalence problem is the difference in aquifers.

The equivalence problems of the VES survey around Chuko are managed using this technique for all other VES curve interpretations.

On the basis of the lithological section from the borehole at Chuko town, the results of the interpretations of the geoelectrical sections at the four profiles (P_o, P_I, P_{II} &P_{VI}) yield the general structure and the fine structure (or the specific arrangement of the strata) as shown in Figures (15), (16), (17) and (18). In general these are described as follows.

The top layer with thickness and resistivity varying in the range respectively from 2 to 6 m and 3 to 500 ohm-m probably has both sedimentary and volcanic origin. The wide range of resistivity variations in these surficial deposits is basically associated with difference in lithological composition. The high moisture content in some of these horizons, the salinity of rocks in the aeration zone and shallow depth of the free ground water level with high salt content are the main causes of the very low resistivity values (less than 10 ohm-m). The intermediate resistivity values are due to surficial deposits with moderate humidity, and these rocks can be water saturated if the depth of the free ground water level is shallow. On the other hand sands of different grain size with low humidity are probably be the causes of high resistivity values (above 100 ohm-m).

Subsurface formations underlying the surficial deposits are represented by rocks of alternative horizons with different electrical resistivities in the range 7-150 ohm-m. The upper part of this layer with thickness 20-40m is composed of volcanic rocks; and the lower part is composed of sedimentary rocks of alternating clay and sand and its depth varies from 20 m in the north west up to 200m and above in other regions. Rocks with resistivity values below 15 ohm-m may be mainly due to clay and ash influences. Increase in resistivity indicates that sand prevails in this layer or may due to increasing size of sandy materials in the layer. The resistivity values in the range from 15-35 ohm-m are due to clay- sand. Resistivities above 50 ohm-m are due to sand, ignimbrites and tuff in the upper part and basically due to sand in the lower part of this layer.

The hydrogeological conditions of the survey area show that a widely distributed drainage system forming deep valley created favorable condition for the flow of ground water to the valley. Both the free ground water and ground water are confined in the underlying horizons, and the depth of the water bearing horizon within the water shade is expected to be thirty meters or above. The presence of these water bearing horizons in the geoelectric sections are indicated by the low electrical resistivity values, but these low resistivity may be due to the variation of the lithological compositions like increase in clay content of the rocks, the presence of mineralized ground water, etc. Incorporating the geological information of the of the borehole and also hydrogeological conditions of the survey area, the results of the VES measurements show that the main water bearing

horizons in the area are sedimentary rocks with resistivity exceeding 40 ohm-m; and this resistivity value seems reasonable for these formations to be saturated with fresh ground water. Specifically, sand is the most saturated with water but its low resistivity value could be due to its high clay content. Moreover, clay-sand and gravely- sand can be fresh ground water saturated. Because of the inhomogenities of the lithological compositions both laterally and with depth, the ground water level determination is somewhat difficult from the present VES information .

On the other hand the stacked section and contour maps of the smoothed resistivity profiling given in figures (11), (13) & (14) show three apparent resistivity sections at the required depth of investigation. The apparent resistivity value is nearly constant at the left side of the base line increases linearly at the middle around the base line and then maintains approximately the peak value with great fluctuations; and finally it tends to drop to the small value that it has at the far left end. In the portions of the curve where the apparent resistivity is nearly constant, we may conclude that the constant apparent resistivity is approximately the same as the true resistivity value for the layer at the depth of investigation.

In general the functional form of the apparent resistivity (in ohm-m) versus the x-values (station positions in meters) along the profile at the measuring depth can be described by the linear equation $\rho_a(x) = ax + b$ where the physical constants a and b can be determined using the least squares approximation. Since a is the slope of the curve, the small or nearly the zero values of a gives $\rho_a(x)$ to be

horizontal line or $\rho_a(x)$ approaches b; and large value of a makes $\rho_a(x)$ nearly to be vertical line. Hence a is related with fault, joint or contact etc. and b is related with the true resistivity of the layer at a given depth so that it has the dimension of resistivity (ohm-m). The constant a has the dimension of resistance (ohm) and it the resistance of the fault zone. If θ is the dip angel of the fault then the relationship between the resistance and the dip angle is given by $a = \tan\theta$. From this the dip angle of the fault in survey area is found to be in between 70^0 and 85^0.

Both constants a and b varies from place to place in a given horizon where the variation of a associated with the structure of rocks and that of b is associated with the content of rocks. Hence it is possible to determine from the measurement of the resistivity at a given depth the content of the rock, the degree of fracturing of the formations and the dipping of the fault in that layer.

As shown in the stacked section of Figure(11) the high resistivity value and the great fluctuations in the right hand side of the base line may be due to the large degree of fracturing of rocks, the linear increase at the middle is due to the lineament structures and the very low constant resistivity value at the left and far end of the right (near 3000E) may be mainly due to the clay influence. Therefore, the profiling analysis confirms the existence of water bearing horizon at nearly the right hand side of the base line with resistivity value in the range from 40 to 100 ohm- m.

3.2. Conclusions and Recommendations

1) The hydrogeological conditions of the survey area show that a widely distributed drainage system form deep valley. This created favorable condition for the flow of groundwater to the valley. The depth of the water bearing horizon within the water shade is expected to be thirty meters or above. Incorporating the geological information of the borehole, the results of the VES measurements show that the main water bearing horizons in the area are sands with varying grain size and fractured volcanic rocks with resistivity exceeding 40 ohm-m; and this resistivity value seems reasonable for these formations to be saturated with fresh groundwater. Because of the inhomogenities of the lithological compositions, the ground water level determination is somewhat difficult from these VES results. Hence to have complete information it is recommended that a detail integrated geological, geophysical and hydrogeological studies be conducted in this general survey area.

2) The geoelectrical sounding curve can yield the information that consist of the data about the number of layers, their thickness, and resistivity values when it is incorporated with an external geological information. The information about the general stratification: about the top layer, the bottom layer, and the possible strata in between can be derived from the VES curve itself without any external information.

The possible strata in between the top and bottom layers are the causes of the equivalence problems. In VES using Schlumberger array, assuming horizontal stratification and other factors such as physical & experimental influences removed, the parts where differences in interpretations occur (i.e. different models to arise) for the VES of Chuko are all aquifers and possibly aquicludes. From the hydrogeological point of view, based on the well known value one can fix the resistivity value of the aquifer at one value for the different models of a given VES curve than to estimate a new one for each model, and then can carry out constrained inversions. The results show that if the horizon bearing water is fixed at one resistivity value, then all those horizons associated with aquifer approximately takes this fixed value after constrained inversion; and it happens that the depth range of aquifer for different models are nearly identical. Hence it is the resistivity value of aquifer but not the number of layers that is important for the interpretation of Schlumberger VES curve for groundwater exploration. We may conclude, in general, that the problem of the principle of equivalence does not alter very much in the interpretation of VES if aquifer is the cause of equivalence.

3) The apparent resistivity versus the station position for the horizon at a given measuring depth can be described mathematically as $\rho_a(x) = ax + b$ where a is the physical constant known as resistance that describes the structure of rocks and b is the physical constant known as the true resistivity that describes the content of rocks at a given horizon having geological meaning thickness.

4) The mathematical formulation and the ways devised to minimize the effects of principle of equivalence are recommended to be further checked by other sets of resistivity data obtained with the help of the more stable resistivity meter unit (preferably the Terameter SAS 300B or SAS 300C unit); and that better topographic conditions with good catchement area is need so as to minimize the influences of horizontal stratification, physical and experimental effects, and the one-to-one relationship between apparent resistivity and thickness and true resistivity hold.

5) In VES using Schlumberger array there are points where the current electrodes separation remain constant but the potential electrodes are changed so as to enhance measurements in potential difference. For this purpose the explorers in the Ethiopian Institute of Geological Surveys (EIGS) usually change MN when MN/AB < 1/3 to collect the data used for this work. However from the theoretical as well as practical point of view, it is very reasonable to change MN when MN/AB < 1/5. In this later case the relationship between MN & AB becomes: for AB/2 = 1.5-30m the value of MN/2 is 0.3m, for AB/2 = 20-220m the value of MN/2 is 4m and for AB/2 = 150-500m the value of MN/2 is 30m. Hence with approximation the geometric factor for symmetrical array and that of Schlumberger array are practically the same.

It has been observed by the author, with the measurement taken using Terrameter SAS 300B unit at Arbaminch water technology Institute, that negligible separation occurs between two apparent values at the same AB/2 but different MN/2 in the case where MN is changed when MN/AB < !/5, and this is also the one recommended in most recent hydrogeological texts.

References

1. Koefoed, O. (1979). Geosounding Principles, 1: resistivity sounding. measurements; Elesevier, Amsterdam
2. Keller, G.V. and Frischknecht, F.C. (1970). Eletrical Methods in geophysical prospecting, pp. 97-187, Pergamon Press, Oxford.
3. Telford, W.M., Geldart, L.P., Sheriff, R.E. and Keys, D.A. Applied Geophysics, pp. 677-686. University Press, Cambridge.
4. Orellana, E. Mooney, H.M. (1966). Master tables and curves for vertical electric sounding over layered structures. Interciencia, Madrid.
5. Verma, R.K., Bhuin, N.C. and Rao, C.V. (1980). Use of electrical resistivity methods for study of some faults in the Jharia Coal field. India, Geoexploration 18, 201- 220.
6. Verma, R.K., and Bandyopadhyay, T.K. (1983). Use of the resistivity method in geological mapping - Case histories from the Raniganj Coal Field, India. Geophysical Prospecting , 31, 490-507.
7. Vozoff, K. (1958). Numerical resistivity analysis: Horizontal layers. Geophysics, 23, 536-556.
8. Kumar, R. (1973b). Resistivity type curve over outcropping vertical dykes-I. Geophysical Prospecting, 21, 560-578.
9. Kumar, R. (1973c). Resistivity type curve over outcropping vertical dyke-II. Geophysical Prospecting, 21, 615-625.

Date June 22/1998

The School of Graduate Studies
Addis Ababa University
Addis Ababa

I certify that the M.Sc. candidate Eyasu Bunaro has incorporated all the necessary comments forwarded by the examination committee of his thesis.

Advisor (TIGISTU HAILE)

Student (EYASU BUNARO)